RM No. E7L02

NACA

RESEARCH MEMORANDUM

INVESTIGATION OF EFFECTS OF SEVERAL FUEL-INJECTION LOCATIONS ON OPERATIONAL PERFORMANCE OF A 20-INCH RAM JET

By W. H. Sterbentz, E. Perchonok
and F. A. Wilcox

Flight Propulsion Research Laboratory
Cleveland, Ohio

NATIONAL ADVISORY COMMITTEE
FOR AERONAUTICS

WASHINGTON
June 8, 1948
Declassified May 16, 1958

NATIONAL ADVISORY COMMITTEE FOR AERONAUTICS

RESEARCH MEMORANDUM

INVESTIGATION OF EFFECTS OF SEVERAL FUEL-INJECTION LOCATIONS ON OPERATIONAL PERFORMANCE OF A 20-INCH RAM JET

By W. H. Sterbentz, E. Perchonok
and F. A. Wilcox

SUMMARY

The results of an investigation conducted in the NACA Cleveland altitude wind tunnel to determine the effects of several methods of fuel injection on the operational performance of a 20-inch ram jet are presented and discussed. Studies were made to pressure altitudes of 35,000 feet and ram-pressure ratios equivalent to supersonic Mach numbers. Four fuel-injection arrangements using the same flame holder were investigated: (1) a fixed amount of fuel injected within the flame holder in a downstream direction and a variable amount of fuel injected near the ram-jet diffuser inlet in an upstream direction; (2) a fixed amount of fuel injected within the flame holder in a downstream direction and a variable amount of fuel injected near the flame holder in an upstream direction; (3) all the fuel injected near the ram-jet diffuser inlet in an upstream direction; and (4) all the fuel injected within the flame holder in a downstream direction. The fuel injected upstream of the flame holder was preheated.

The blow-out limits and the combustion stability of each fuel-injection arrangement were determined. In addition, the effects of fuel-air ratio, combustion-chamber-inlet velocity, combustion-chamber-inlet static pressure, and ambient-air pressure on combustion efficiency are presented and analyzed. Engine performance results obtained for the 20-inch ram jet with a 17-inch-diameter exhaust nozzle and one of the fuel-injection arrangements investigated are also presented.

Changes in the location of the point of fuel injection with respect to the flame holder proved to be very important to the performance of the combustion chamber. Pronounced variation in combustion efficiency with changes in either combustion-chamber-inlet

velocity or over-all fuel-air ratio was noted. The range of fuel-air ratios over which combustion could be maintained was decreased when the engine was operated close to the conditions of ram for which choking occurs at the exhaust nozzle. The full fuel-air ratio range of operation however was recovered after the engine was choked.

INTRODUCTION

One of the difficult phases of ram-jet combustion-chamber development is the problem of obtaining stable combustion of high efficiency over a wide range of fuel-air ratios, combustion-chamber-inlet velocities, and altitudes. Combustion studies reported in references 1 to 3 have shown the importance of the method of fuel injection on the performance of the ram-jet combustion chamber. From these experiments, in which all the fuel was injected upstream of the flame holder, burners that operated to high altitudes and to pressure ratios corresponding to supersonic Mach numbers were developed at the NACA Cleveland laboratory (references 1, 4, and 5). The flame holders of some burners of this type would, however, support combustion only at low combustion-chamber-inlet velocities or over narrow ranges of fuel-air ratios. In addition, combustion was sometimes accompanied by undesirable vibrations at frequencies ranging from 25 to 125 cycles per second.

An investigation was conducted in the NACA Cleveland altitude wind tunnel to determine the effects of several methods of fuel injection on the operational performance of a 20-inch ram jet. The location of the point of fuel injection with respect to the flame holder was thought to be important in the performance of flame holders. In this study, the effects on ram-jet combustion-chamber performance of four fuel-injection arrangements, which used the same flame holder, were investigated (fig. 1).

For each configuration, the quantitative effects of fuel-air ratio, combustion-chamber-inlet velocity, combustion-chamber-inlet static pressure, and ambient-air static pressure on combustion efficiency are presented. The effect of exhaust-nozzle-outlet diameter and exhaust-nozzle choking on the fuel-air-ratio operating range is indicated for the configuration using the split-injection burner. The performance results for the 20-inch ram jet with a 17-inch exhaust nozzle and an 8-foot combustion chamber using this burner were investigated and are presented.

APPARATUS AND PROCEDURE

The investigation was made with a ram jet having a subsonic conical diffuser, a constant-area combustion chamber, and a converging exhaust nozzle (fig. 2). The diffuser had an 8° included angle, a 14-inch-diameter inlet, and a 20-inch-diameter outlet. A converging nozzle 2 feet long with either a 15-inch- or a 17-inch-diameter outlet was attached to the 8-foot combustion chamber. The construction of the water-cooled combustion chamber and exhaust nozzle was similar to the experimental combustion chamber described in reference 5. These sections were made by seam-welding a corrugated outer shell to a smooth inner shell to form a helical cooling-water path.

The four fuel-injection arrangements were: (1) a fixed amount of fuel injected within the flame holder in a downstream direction and a variable amount of fuel injected upstream of the flame holder near the ram-jet diffuser inlet in an upstream direction (split-injection burner, fig. 1(a)); (2) a fixed amount of fuel injected within the flame holder in a downstream direction and a variable amount of fuel injected at the flame holder in an upstream direction (flame-holder split-injection burner, fig. 1(b)); (3) all fuel injected upstream of the flame holder near the ram-jet diffuser inlet in an upstream direction (upstream-injection burner, fig. 1(c)); and (4) all fuel injected within the flame holder in a downstream direction (flame-holder injection burner, fig. 1(d)).

Two independent fuel systems were used: one for the upstream fuel injectors and one for the fuel injector within the flame holder. The fuel injected in an upstream direction was preheated. The preheating system consisted of a heat exchanger using saturated steam at a pressure of 100 pounds per square inch gage as the heating medium (reference 4). The preheated fuel temperature was maintained at 200° ± 10° F. With the split-injection arrangements, the fuel flow within the flame holder was maintained constant at 1000 pounds per hour for all operating conditions and the fuel temperature was approximately 80° F. Unleaded 62-octane fuel (AN-F-22) was used in this study.

For all arrangements of the fuel-injection systems, the flame holder used (fig. 3) was a modification of the annular V type B burner described in reference 1. It consisted of two perforated annuli of 9- and 16-inch center-line diameters, and a perforated center cone. Both annuli and the center cone had a 30° V cross-section with a 3-inch chord. For the injection of fuel downstream within the flame holder, 32 equally spaced 6-gallon-per-hour commercial spray nozzles

were provided in the outer annulus, 16 equally spaced 6-gallon-per-hour commercial spray nozzles in the inner annulus, and one 21.5-gallon-per-hour spray nozzle in the center cone. These nozzles were the 60° hollow-cone type and were fed from a single fuel source. Additional radial gutters were welded between the annuli and the cone to improve its flame-holding characteristics. The total-pressure drop of this flame holder was 1.5 times the combustion-chamber-inlet dynamic pressure.

For fuel injection in an upstream direction at the flame holder, 18 commercial spray nozzles were provided in front of the outer annulus, 12 commercial spray nozzles were provided in front of the inner annulus, and one commercial spray nozzle was provided in front of the center cone. These nozzles were rated to deliver 21.5 gallons of fuel per hour in the form of a 60° hollow cone at a pressure of 100 pounds per square inch gage. All nozzles were fed from a single fuel source. This fuel injector, which is mounted just upstream of the flame holder in the combustion-chamber-inlet section, is shown in figure 4.

The fuel injector used in the studies requiring fuel injection upstream of the flame holder near the diffuser inlet is shown in figure 5. This fuel injector consisted of six $\frac{5}{16}$-inch tubes arranged in an 80° V pattern in which the open end of the V is 5 inches downstream of the diffuser inlet. The fuel was sprayed in an upstream direction. Previous investigations in which preheated fuel was used (references 4 and 5) indicated the necessity of maintaining a fuel-manifold pressure greater than the fuel vapor pressure and the desirability of a fuel injector that would permit a wide range of fuel flows with small variation in fuel pressure. Such a system is impossible with a fixed-orifice-area injector, but can be accomplished with a variable-orifice-area injector. The fuel injector was designed accordingly and consisted of two concentric tubes arranged to permit relative displacement of one with respect to the other. The outer tube had a series of 0.028-inch holes drilled along its length and the inner tube had a series of slots along its length opposite the orifices in the outer tube. A small displacement of the inner tube made possible a variation in the total number of open orifices from 18 to 144 in eight equal steps. The orifices and slots were located to give a uniform fuel distribution at each setting. The aerodynamic total-pressure drop of the fuel injector was 0.54 times the dynamic pressure at the combustion-chamber inlet.

Ignition for the cases in which fuel was injected within the flame holder was accomplished by means of a modified aircraft spark

plug. When all the fuel was injected upstream of the flame holder, a gas pilot, which was built into the flame holder, was required to start combustion. Ignition of the gas pilot was also accomplished by means of the modified aircraft spark plug.

Dry refrigerated air at approximately sea-level pressure was made available to the ram jet through a make-up air duct and was throttled to provide the desired static pressure at the combustion-chamber inlet. The engine exhausted directly into the wind-tunnel test section where the pressure altitude was varied to the desired condition. A 7-foot chord wing supported by the wind-tunnel balance frame served as a mounting for the ram jet. The wind-tunnel balance system was used to measure the thrust. Free movement of the model was obtained by a sealed slip joint inserted between the ram jet and the make-up air duct. Thrust values calculated from data obtained with a water-cooled exhaust rake (fig. 2), which are not presented, were consistent with values obtained with the wind-tunnel balance.

The engine operational performance was investigated at various ambient-air pressures from 1450 to 500 pounds per square foot absolute. The inlet-air temperature was maintained at $10^{\circ} \pm 10^{\circ}$ F. At each ambient-air pressure, readings were taken over a range of combustion-chamber-inlet static pressures at intervals of 100 pounds per square foot. Data were thus obtained at various pressure altitudes and ram-pressure ratios. At each combustion-chamber-inlet static pressure and altitude, the fuel-air ratio was varied over the range at which combustion could be maintained.

Total pressures, static pressures, and indicated temperatures measured at the diffuser inlet were used to compute the air flow. From these measurements and an additional measurement of static pressure at the combustion-chamber inlet, combustion-chamber-inlet velocities were computed. Rotameters were used to measure the fuel flow. Combustion efficiency and gas temperature rise were computed from measured values of jet thrust and gas flow by the methods presented in references 1 and 5. The heat lost to the combustion-chamber cooling water was accounted for in the calculation of combustion efficiency. This heat loss was computed from cooling-water flow and temperature-rise measurements.

The engine performance parameters were computed by methods discussed in references 1 and 5. For equivalent free-stream Mach number values less than 1, the diffuser-inlet total pressure was taken as the equivalent free-stream total pressure in computing Mach number; for values greater than 1, supersonic diffuser losses

were added to the measured subsonic diffuser-inlet total pressure to obtain the equivalent free-stream total pressure. The losses were assumed to be those that would occur across a normal shock at the throat of a convergent-divergent supersonic diffuser of optimum contraction (reference 5).

SYMBOLS

The following symbols are used in this report:

A	cross-sectional area, square feet
C_F	net-thrust coefficient, $\frac{2 F_n}{\gamma_0 p_0 A_3 M_0^2}$
F_j	jet thrust, pounds
F_n	net thrust, pounds
f/a	fuel-air ratio
M	Mach number
p	static pressure, pounds per square foot absolute
T	total temperature, $^{\circ}R$
V	velocity, feet per second
W_a	air flow, pounds per second
W_f	fuel flow, pounds per hour
γ	ratio of specific heat at constant pressure to specific heat at constant volume
δ	ratio of absolute tunnel ambient-air pressure to absolute static pressure at NACA standard atmospheric conditions at sea level, $p_0/2116$
η	over-all efficiency, percent
η_b	combustion efficiency, percent

θ ratio of absolute total temperature at diffuser inlet to absolute static temperature at NACA standard atmospheric conditions at sea level ($T_0 = T_1$), $T_0/519$

τ ratio of absolute total temperature at exhaust-nozzle outlet to absolute total temperature at diffuser inlet, T_4/T_1

Subscripts:

0 equivalent free-stream condition

1 subsonic-diffuser inlet

2 diffuser outlet and combustion-chamber inlet

3 combustion-chamber outlet

4 exhaust-nozzle outlet

RESULTS AND DISCUSSION

The variation of combustion efficiency η_b with either combustion-chamber-inlet velocity V_2 or over-all fuel-air ratio f/a was greatly affected by the following three factors: (1) fuel atomization, (2) degree of fuel stratification, and (3) time allowed for combustion. Changes in the fuel-injection arrangements changed the effects of these variables on the combustion efficiency. Because of the nature of the investigation, independent control of all the experimental variables was not feasible. All the experimental conditions at which the data were obtained are therefore given for each of the different configurations. Certain of these variables have little effect on the combustion-chamber performance, as will be shown.

The effects on η_b of the fuel-injection arrangements are presented over a range of operating variables in figures 6 and 7. Figure 6 presents η_b plotted against V_2 for the split-injection burner, the upstream-injection burner, and the flame-holder injection burner. These data were obtained with a 17-inch-diameter exhaust nozzle. The gas total-temperature ratios across the engine τ that were attained, the combustion-chamber-inlet static pressures p_2, and the ambient-air pressures p_0 at which the data were taken are also given. Data are presented at approximately constant f/a for each burner. The fuel-air ratios selected are the values at which

the maximum range of operating variables was obtained. An evaluation of the effect of V_2 upon η_b at a constant f/a for the flame-holder split-injection burner is not presented because sufficient data were not obtained for such an analysis.

With the split-injection burner operating at a f/a value of 0.040 ± 0.002 an increase in η_b from 45 to 81 percent was obtained as V_2 was increased from 96 to about 138 feet per second. (See fig. 6(a).) This marked increase in η_b was largely due to the more complete atomization and mixing with air of the fuel injected from the upstream fuel injector (fig. 5) that occurs as V_2 is increased. The improvement in fuel dispersion and atomization with increased V_2 occurs because the fuel is ejected in fine streams through simple orifices against the direction of air flow. The greater the relative velocity of the air over the fuel streams the greater is the tearing action of the air on the fuel (reference 6).

A sharp reversal in trend occurs at a V_2 value of about 140 feet per second, the value at which peak combustion efficiency (η_b, 81 percent) was obtained, and further increases in V_2 result in a gradual decrease in η_b. Presumably the improvement in fuel atomization and fuel-air mixing with further increases in V_2 did not increase η_b sufficiently to overcome the loss in η_b that results from the decreased time available for combustion at higher V_2 values. The combined effect produces a gradual decrease in η_b with increases in V_2 above values of 140 feet per second (fig. 6(a)). The maximum velocity shown on this figure was limited by choking at the exhaust nozzle of the engine and not by combustion blow-out.

At an approximately constant value of V_2, variations in p_2 over the range investigated (1200 to 2000 lbs/sq ft absolute) had little effect on η_b. Variations in p_0 over the range investigated at fixed values of V_2 also show little effect on η_b.

The variation of τ with V_2 follows the pattern of the variation of η_b with V_2. An approximate peak value of τ of 5.5 was attained at a value of V_2 of 140 feet per second, the same value of V_2 at which the peak η_b occurred.

The variation of η_b with V_2 at a f/a value of 0.055 ± 0.001 for the upstream-injection burner is shown in figure 6(b). As with the split-injection burner, η_b rapidly increased with increases in V_2, reaching a peak of 78 percent at about 140 feet per second.

Further increases in V_2 resulted in a gradual decrease in η_b. The same trend might be expected with this burner as with the split-injection burner because the same upstream fuel injector was used in both studies.

When all the fuel was injected within the flame holder, a decrease in η_b occurred with increases in V_2. This variation at a f/a value of 0.020 $\pm$ 0.001 is shown in figure 6(c). For an increase in V_2 from 117 to 177 feet per second, η_b decreased from 68 to 47 percent. This drop in η_b was probably caused by the reduced time available for combustion with increased V_2. There could be little effect upon the fuel atomization or fuel-air mixing with changes in V_2 as when fuel was injected from the upstream injector, because the fuel spray nozzles are shielded within the flame holder. For the data obtained, the fuel pressure was maintained at a high value to minimize its effect on fuel atomization.

Combustion efficiency η_b plotted against over-all fuel-air ratio f/a is presented in figure 7 for the split-injection burner, the upstream-injection burner, the flame-holder split-injection burner, and the flame-holder injection burner. As with the data presented in figure 6, these data were obtained for the burners operated with a 17-inch-diameter exhaust nozzle. The gas total-temperature ratios across the engine τ that were attained and the combustion-chamber-inlet velocities V_2 and static pressures p_2 at which the data were taken are also shown. Data are presented at a value of p_0 of 1450 pounds per square foot absolute.

The range of f/a for stable combustion with the split-injection burner was from approximately 0.033 to 0.050. (See fig. 7(a).) At a given value of p_2, the η_b gradually increased with f/a until a maximum was reached at a f/a value of approximately 0.044. Further increases in f/a decreased η_b. The increase in η_b with f/a is partly due to the increased concentration of fuel, thereby improving conditions that lead to more rapid chemical reaction. Primarily because a zone of rich fuel-air mixtures was maintained at the flame-holder gutters, the maximum η_b occurred at less than stoichiometric over-all f/a (0.067). As the over-all value of f/a was increased beyond 0.045, local overenrichment at the flame holder occurred and the excess fuel in this zone would not burn to completion regardless of how favorable were the conditions for combustion.

The variation in η_b with f/a, as shown in figure 7(a), is also affected by the V_2 at which the data were taken. Inasmuch as the data in figure 6(a) have shown that p_2 had little effect

on η_b, the apparent change in η_b with p_2 shown in figure 7(a) actually arises from the variation in V_2 caused by changes in p_2. For the split-injection burner, η_b decreases as f/a is increased to values greater than 0.045. At the same time, the value of τ continues to increase over the f/a range of stable burning shown in figure 7(a).

When only upstream injection was used, a displacement in the f/a range over which combustion could be maintained occurred, as shown in figure 7(b). Peak η_b occurred at a f/a value of approximately 0.062 and flame blow-out occurred at values of f/a below 0.055 and above 0.068. The shift in peak η_b to richer f/a values by changing from split injection to full upstream injection is primarily due to reduced fuel stratification. As a result of a more uniform fuel-air mixture over the combustion-chamber cross section, maximum η_b occurred at a fuel-air ratio nearer stoichiometric.

The range of f/a over which combustion could be maintained with the flame-holder split-injection burner is presented in figure 7(c). The combustion efficiency η_b increased rapidly with f/a until the maximum was reached at a value of 0.040. Because all the fuel is concentrated at the flame-holder gutters, the peak η_b would be expected to occur at a leaner over-all fuel-air ratio than for the split-injection burner or for the upstream-injection burner. When f/a was increased beyond 0.040, a rapid decrease in η_b occurred, the drop being sufficient to cause a slight decrease in the value of τ that was obtained. Blow-out occurred at f/a values below 0.031 and above 0.047.

Data obtained with the flame-holder injection burner were limited by the fuel flow obtainable through the fixed-area orifices of the spray nozzles used. As a result, neither the entire range of fuel-air ratios over which combustion could be maintained nor the peak η_b with fuel-air ratio was determined. The data which were obtained for this burner are shown in figure 7(d).

As the fuel-air ratio was increased from 0.012, which was the leanest f/a at which combustion was maintained with the flame-holder injection burner, η_b increased (fig. 7(d)). The increased η_b was caused in part by the increased concentration of fuel in the fuel-air mixture and in part by the decrease in V_2 that occurred as the exhaust-nozzle-outlet temperature increased with f/a. This decrease in V_2 allowed more time for combustion.

The fuel-air ratio at which the peak combustion efficiency occurred was not determined, but a f/a value as high as 0.046 was obtained, at which point the highest measured η_b (89 percent) occurred. This point is well past the f/a value of 0.040 and a little past the f/a value of 0.045 established as the values at which maximum η_b was attained with the flame-holder split-injection burner and the split-injection burner, respectively.

The location of the point of fuel injection with respect to the flame holder proved to be very important to the operational performance of the combustion chamber. When all the fuel was injected upstream of the flame holder near the diffuser inlet, unsatisfactory performance of the combustion chamber resulted. Although flame filled the combustion chamber, burning was accompanied by severe and irregular vibrations over the entire range of operation. Burning ceased when the ram-pressure ratio across the engine was increased to 2.12, corresponding to an equivalent free-stream Mach number M_0 of 1.10. This value of ram-pressure ratio was just under that required to choke the engine at the exhaust nozzle.

When the split-injection system was used, the severe, irregular vibration was eliminated except near the fuel-air ratio blowout limits. In addition to stabilizing combustion, the burner operated at a ram-pressure ratio of 4.06, corresponding to an equivalent free-stream Mach number of 1.60. (This limit was set by the pumping capacity of the wind-tunnel exhausters.) Flame completely filled the combustion chamber over the range of fuel-air ratios at which combustion could be maintained. At low combustion-chamber-inlet velocities, spark ignition was possible at pressure altitudes of 25,000 feet. As with other burners (reference 5) when the engine was choked at the exhaust nozzle, operation of the engine was independent of variations in tunnel ambient-air pressure.

Stable combustion was also obtained when all the fuel was injected within the flame holder; because of the fixed-area orifices of the spray nozzles, however, operation of the burner was limited to the maximum fuel flow that could be obtained. This burner did not support combustion at ram-pressure ratios greater than 1.28, which is considerably below that required to choke the engine. This value of ram-pressure ratio corresponds to a M_0 value of 0.595.

Combustion was unsteady with the flame-holder split-injection burner. The burner was operated to a ram-pressure ratio of 2.51 before the instability of combustion rendered the burner inoperative. This value of ram-pressure ratio corresponds to a M_0 of 1.23.

The range of f/a over which combustion could be maintained was affected when a change in the outlet diameter of the exhaust nozzle was made. This effect is shown in figure 8, which presents data obtained with the split-injection burner operating with a 17-inch- and a 15-inch-diameter exhaust nozzle for a fixed value of p_0 and narrow range of p_2. The values of τ attained and the values of V_2 at which the data were obtained are also presented.

A range of f/a from 0.025 to 0.068 was obtained with the 15-inch-diameter exhaust nozzle. The range with a 17-inch nozzle was from 0.033 to 0.048. Although the range of f/a was narrower when the 17-inch nozzle was used, higher values of η_b were attained with this nozzle. At any given f/a, a higher value of η_b was obtained with the 17-inch nozzle; larger values of V_2 were obtained with increased nozzle-outlet area, and for the range of V_2 at which these data were taken, η_b increased with V_2. Concomitant increases in τ were also obtained with the 17-inch nozzle because of the improved η_b.

The effect of choking at the exhaust nozzle on η_b, V_2, τ, and the range of f/a at which combustion could be maintained is shown in figure 9. Data are presented for the split-injection burner operating in the combustion chamber with a 17-inch-diameter exhaust nozzle. For this configuration, exhaust-nozzle choking occurred at M_0 of 1.13. Below choking at any given f/a (figs. 9(a) and 9(b)), η_b increased with increases in ram-pressure ratio across the engine. As previously discussed, the primary cause for the higher values of η_b at any given f/a is the increase in V_2 that accompanies the increase in ram-pressure ratio. An increase in τ results from the increase in η_b.

As the ram-pressure ratio across the engine is further increased to values in the neighborhood of choking at the exhaust nozzle (fig. 9(b)), a noticeable decrease in the f/a range of operation is indicated. The range of f/a was recovered, however, after the engine was fully choked (figs. 9(c) and 9(d)). After the engine had been choked, changes in p_0 did not affect the range of f/a, and at a given f/a did not affect η_b, V_2, nor τ. The peak η_b occurred at approximately the same f/a and was independent of the other operating variables.

Because the split-injection burner had desirable combustion characteristics, the performance of the ram jet with this burner was investigated. The results of this investigation are presented in figures 10 to 16. The relations with the free-stream Mach number of the ram-jet performance parameters, reduced jet thrust F_j/δ, reduced net thrust F_n/δ, net-thrust coefficient C_F, reduced air flow $W_a\sqrt{\theta}/\delta$, over-all efficiency η, and specific fuel consumption W_f/F_n are shown in figures 11 to 16, respectively, for the engine with a 17-inch-diameter exhaust nozzle and the split-injection burner. These parameters were computed by methods discussed in references 1 and 5.

At a given flight condition, the f/a at which the ram jet is operated will determine the C_F and η of the engine. Figure 10 shows η_b, η, C_F, and τ plotted against f/a for the ram jet with a 15-inch-diameter exhaust nozzle and the split-injection burner at an M_0 of 1.08. The over-all efficiency η improves with increases in f/a to a maximum value of 5.9 percent at a f/a of approximately 0.042. This rise in η with f/a is primarily caused by the increase in η_b with f/a. Increases in f/a greater than that at which the peak η occurred resulted in a sharp loss in η. This loss is due partly to the decrease in η_b and partly to the continued increase in τ. The following equation shows that η is a direct function of η_b and an inverse function of τ, which causes η to drop with decreases in η_b and increases in τ:

$$\eta = \frac{(\gamma_0-1)\,M_0^2}{1+\frac{\gamma_0-1}{2}M_0^2}\left(\frac{\eta_b}{1+\sqrt{\tau}}\right) \qquad (1)$$

Equation (1) was derived in reference 5 as equation (10).

Because τ continues to increase with f/a, C_F increases with f/a. Increasing f/a from 0.030 to 0.065 resulted in an increase in τ from 3.3 to 6.2 and an increase in C_F from 0.33 to 0.49.

Jet thrust, net thrust, net-thrust coefficient, and air flow increased with M_0 (figs. 11 to 14, respectively). The maximum jet thrust developed, reduced to sea-level conditions, F_j/δ was

10,750 pounds at a M_0 of 1.60. The corresponding F_n/δ was 5940 pounds and the C_F was 0.72. At these conditions, the air flow through the engine was 106 pounds per second reduced to sea-level conditions.

An improvement in η and net specific fuel consumption W_f/F_n (figs. 15 and 16, respectively) were obtained with increased M_0. At $M_0 = 1.60$, $\tau = 4.5$, and $\eta_b = 80.5$ percent, the maximum η was 12.9 percent (fig. 15). The corresponding net specific fuel consumption (fig. 16) was 2.7 pounds of fuel per hour per pound of net thrust. No curves have been drawn through the data because variations in η_b and τ caused the data to scatter. Single curves of η and W_f/F_n can be obtained if η_b and τ are included in a parameter, as suggested in reference 5.

SUMMARY OF RESULTS

From an investigation to determine the effect of various fuel-injection locations with respect to the flame holder on the performance of a 20-inch ram jet, the following results were obtained:

1. The location of the point of fuel injection with respect to the flame holder was very important to the performance of the flame holder and the combustion chamber. With the flame holder used in this investigation, unstable combustion was encountered when either the upstream-injection or flame-holder split-injection systems were used; whereas stable combustion was obtained with either the split-injection or flame-holder injection arrangements.

2. With the arrangements and methods of fuel injection employed in this investigation, pronounced variation in combustion efficiency with changes in combustion-chamber-inlet velocity was noted. For both the split-injection and the upstream-injection burners, the combustion efficiency increased with increases in combustion-chamber-inlet velocity to a value of about 140 feet per second. Further increases in combustion-chamber-inlet velocity resulted in a gradual decrease in combustion efficiency. When all the fuel was injected within the flame-holder gutters, the combustion efficiency decreased with an increase in combustion-chamber-inlet velocity.

3. At an approximately constant combustion-chamber-inlet velocity, data obtained with the split-injection burner indicate that variations in combustion-chamber-inlet static pressure over the range investigated (1200 to 2000 lb/sq ft absolute) had little effect on the combustion efficiency. Variations in ambient-air static pressure over the range investigated at fixed values of combustion-chamber-inlet velocity also show little effect upon combustion efficiency.

4. The range of fuel-air ratios over which combustion can be maintained was decreased when the engine was operated close to the conditions of ram at which choking occurs at the exhaust nozzle. The full fuel-air-ratio range of operation was recovered, however, after the engine was fully choked.

Flight Propulsion Research Laboratory,
National Advisory Committee for Aeronautics,
Cleveland, Ohio.

REFERENCES

1. Perchonok, Eugene, Wilcox, Fred A., and Sterbentz, William H.: Preliminary Development and Performance Investigation of a 20-Inch Steady-Flow Ram Jet. NACA ACR No. E6D05, 1946.

2. Peterson, C., and DeVault, R. T.: Subsonic Ram Jet Development of the Marquardt Aircraft Co. C-20-.85 Ram Jet Engine. (Summary Report) USCAL Rep. No. 2, Univ. Southern Calif., Dec. 1, 1945. (Revised March 15, 1946.)

3. Bevans, R. S., Shipman, J. J., Smith, F. W., and Williams, G. C.: Subsonic Ram Jet Combustion Chamber Program. (Summary Report) DIC 6201, Jet Propulsion Combustion Chamber Res., M.I.T., April 16, 1945.

4. Perchonok, Eugene, Wilcox, Fred A., and Sterbentz, William H.: Investigation of the Performance of a 20-Inch Ram Jet Using Preheated Fuel. NACA RM No. E6I23, 1946.

5. Perchonok, Eugene, Sterbentz, William H., and Wilcox, Fred A.: Performance of a 20-Inch Steady-Flow Ram Jet at High Altitudes and Ram-Pressure Ratios. NACA RM No. E6L06, 1947.

6. Lee, Dana W., and Spencer, Robert C.: Photomicrographic Studies of Fuel Sprays. NACA Rep. No. 454, 1933.

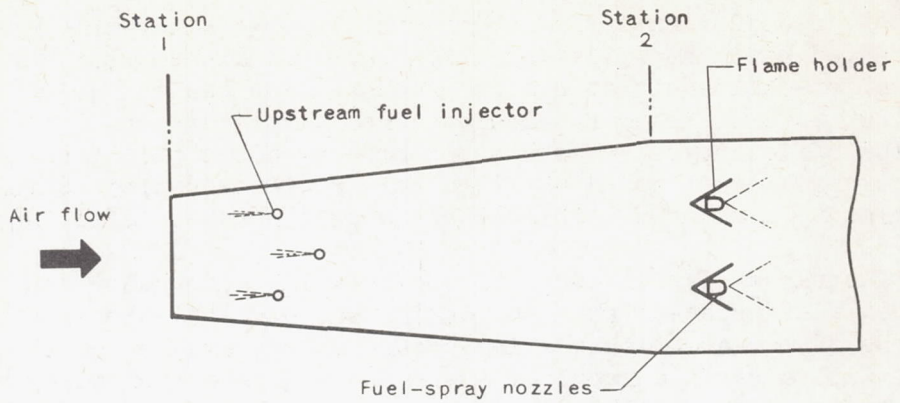

(a) Split-injection burner.

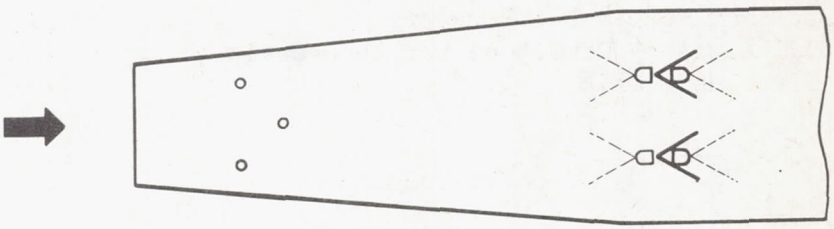

(b) Flame-holder split-injection burner.

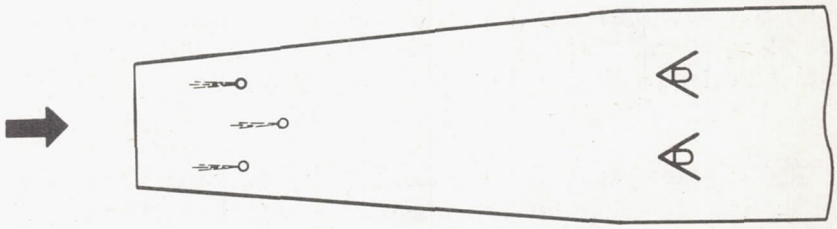

(c) Upstream-injection burner.

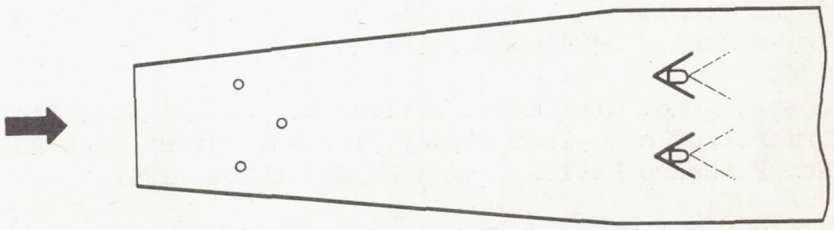

(d) Flame-holder injection burner.

Figure 1. - Schematic diagrams illustrating fuel-injection arrangements used in operational performance investigation of 20-inch ram jet.

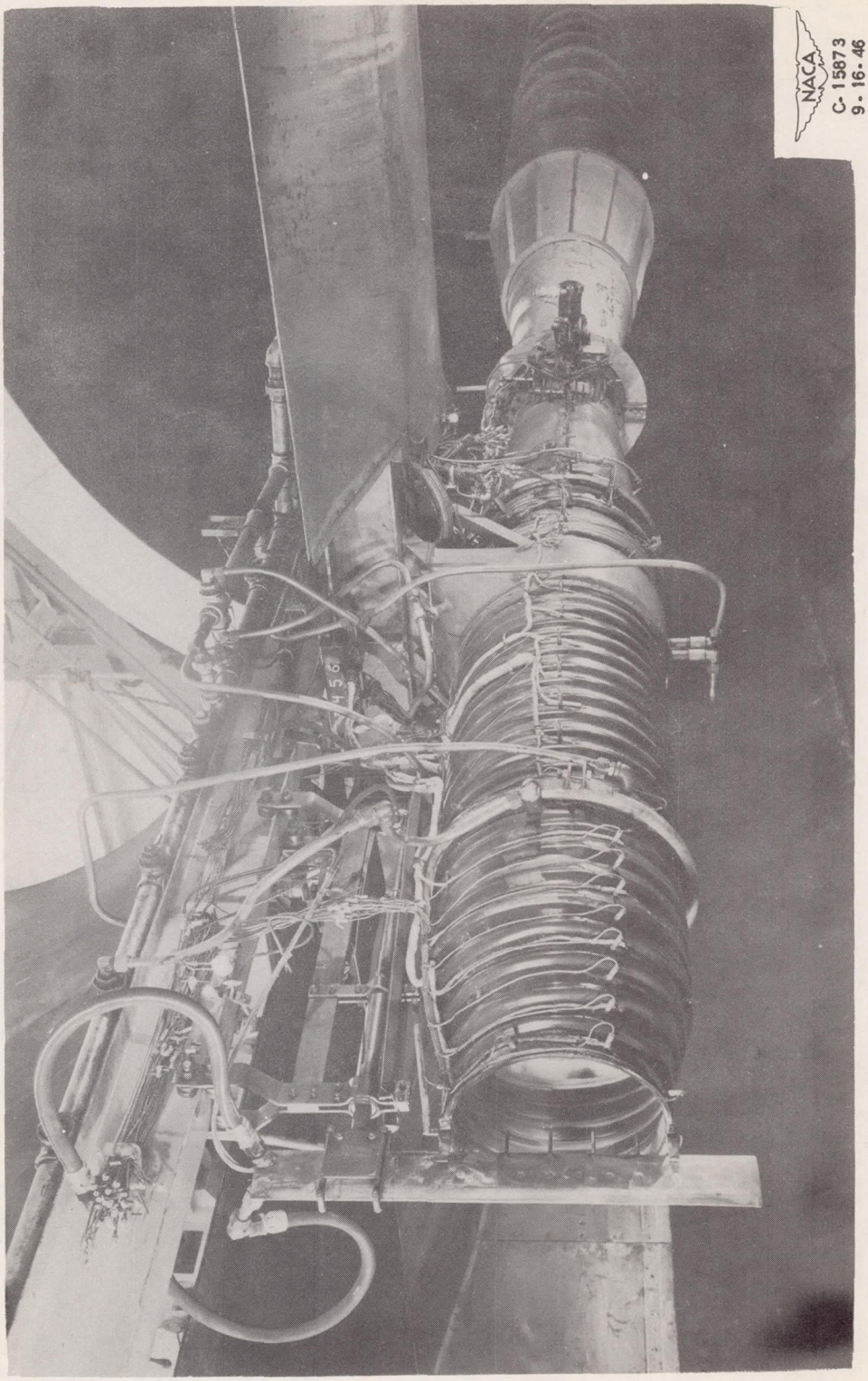

Figure 2. - Installation of 20-inch ram jet in altitude wind tunnel.

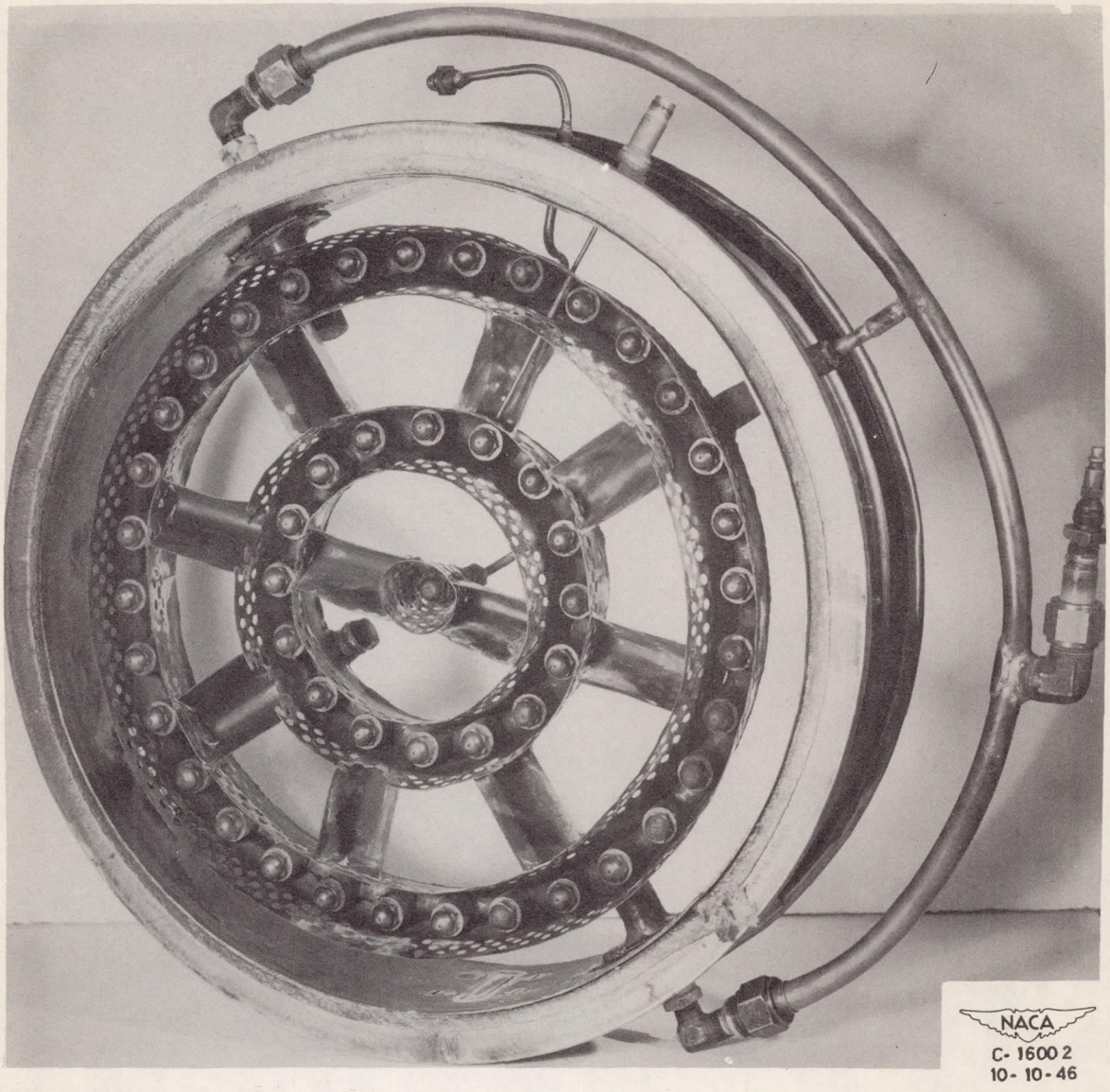

Figure 3. - Downstream view of flame holder showing spray nozzles within flame-holder gutters.

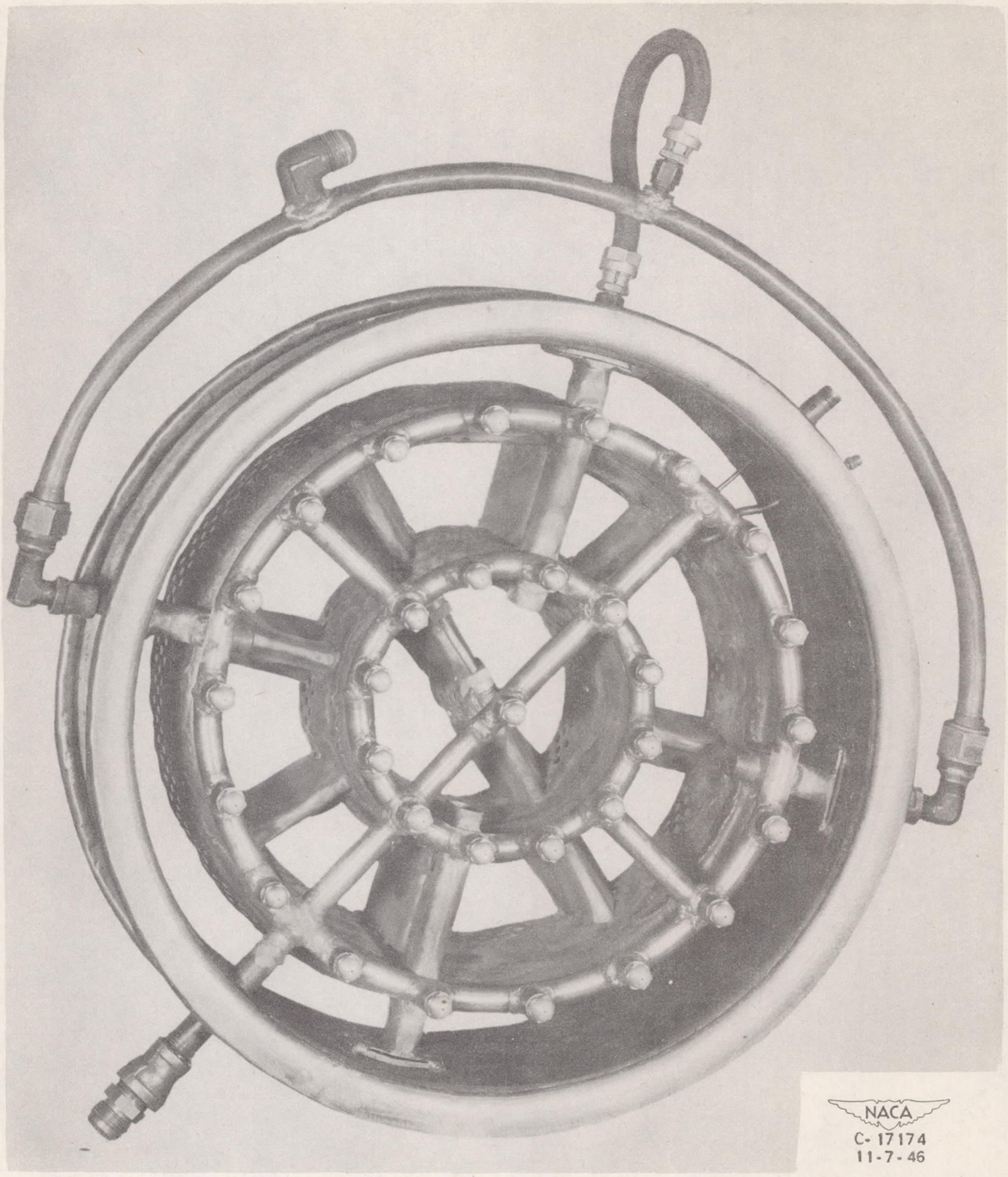

Figure 4. - Fuel injector used in investigations requiring injection of fuel at flame holder in upstream direction.

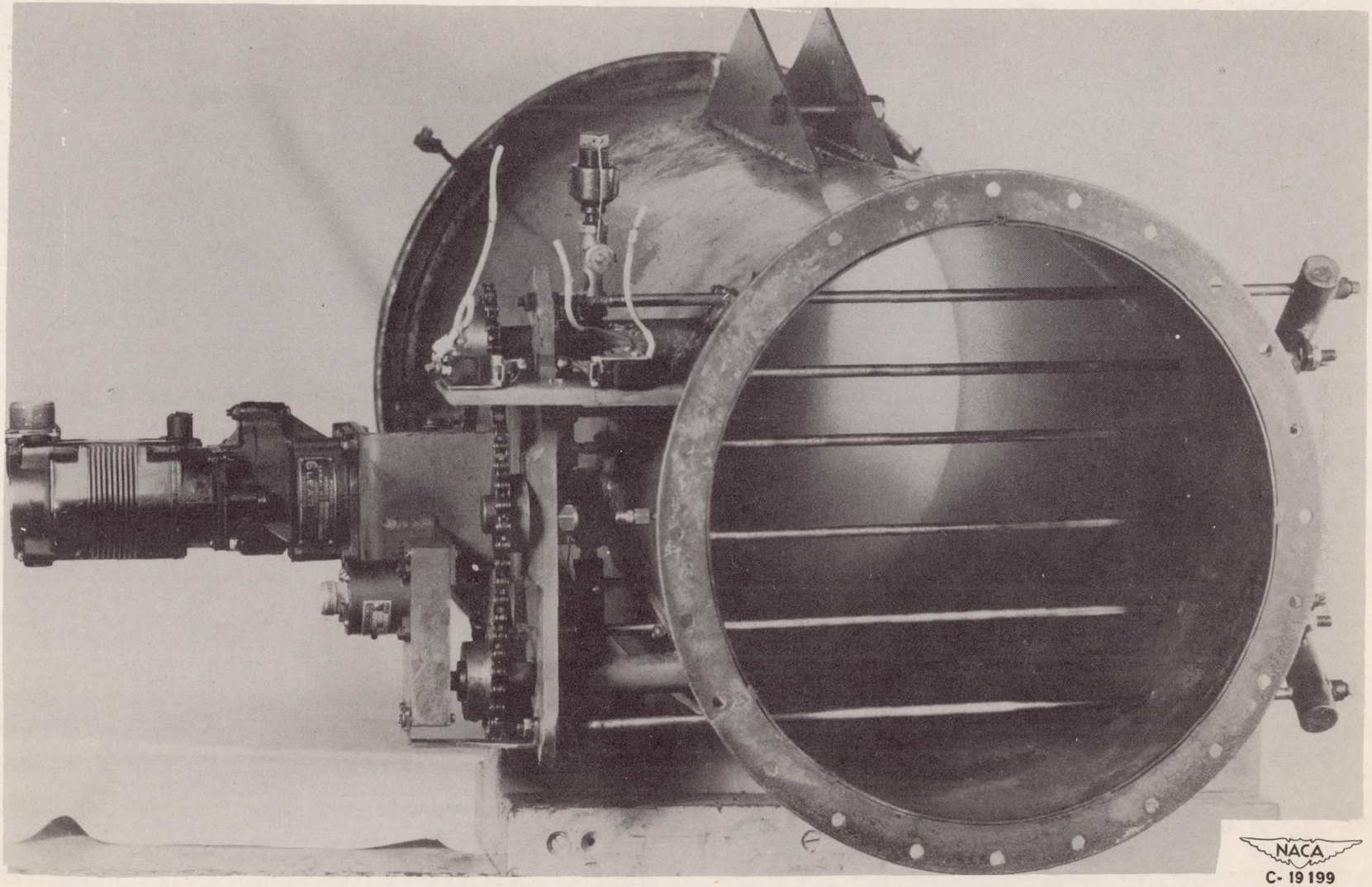

Figure 5. - Upstream view of six-tube injector used in studies requiring injection of fuel near ram-jet diffuser inlet.

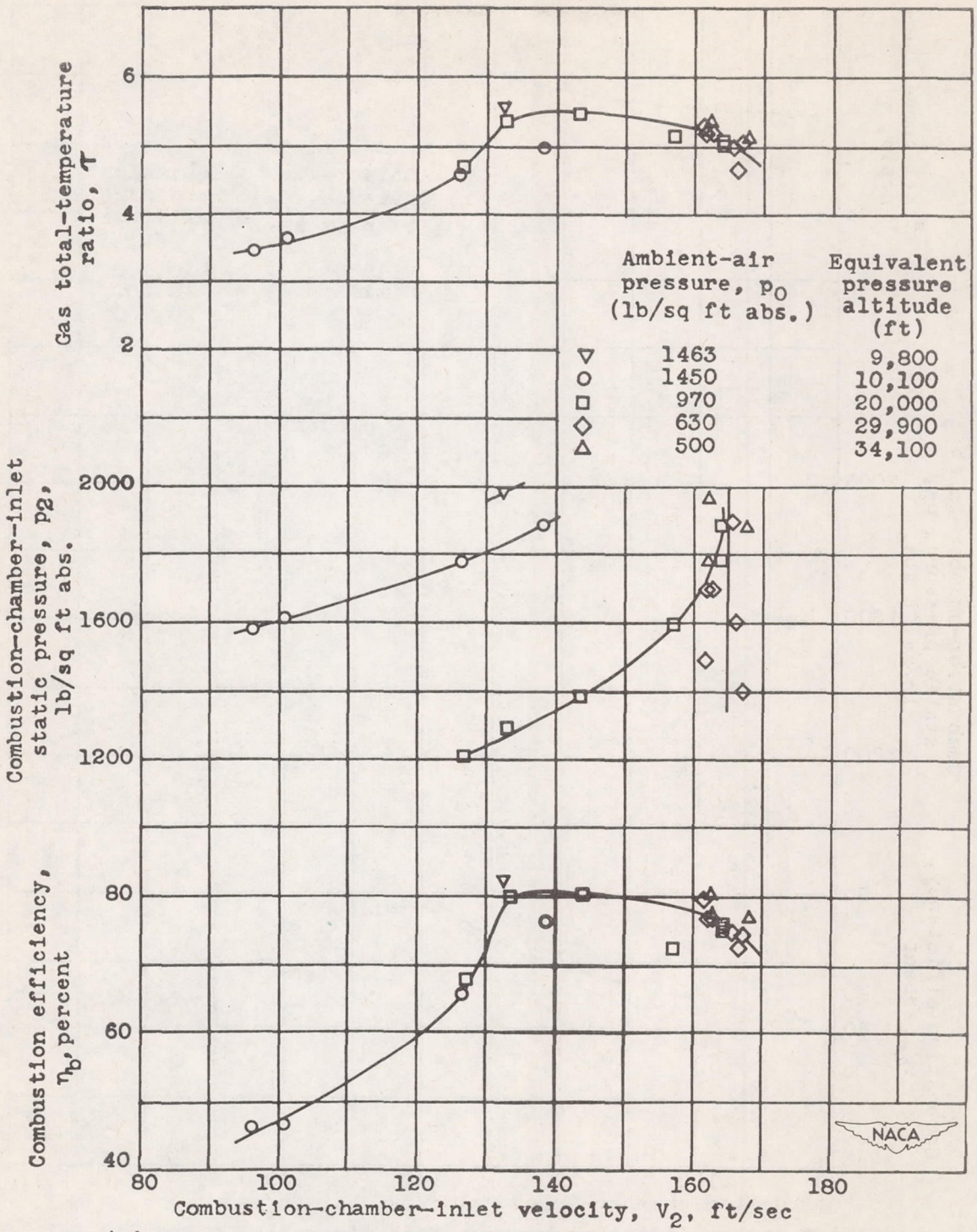

(a) Split-injection burner; fuel-air ratio, 0.040 ± 0.002.

Figure 6. - Effect of combustion-chamber-inlet velocity on combustion efficiency and gas total-temperature ratio at various conditions of ambient-air pressure and combustion-chamber-inlet static pressure. 20-inch ram jet with 8-foot combustion chamber and 17-inch-diameter exhaust nozzle.

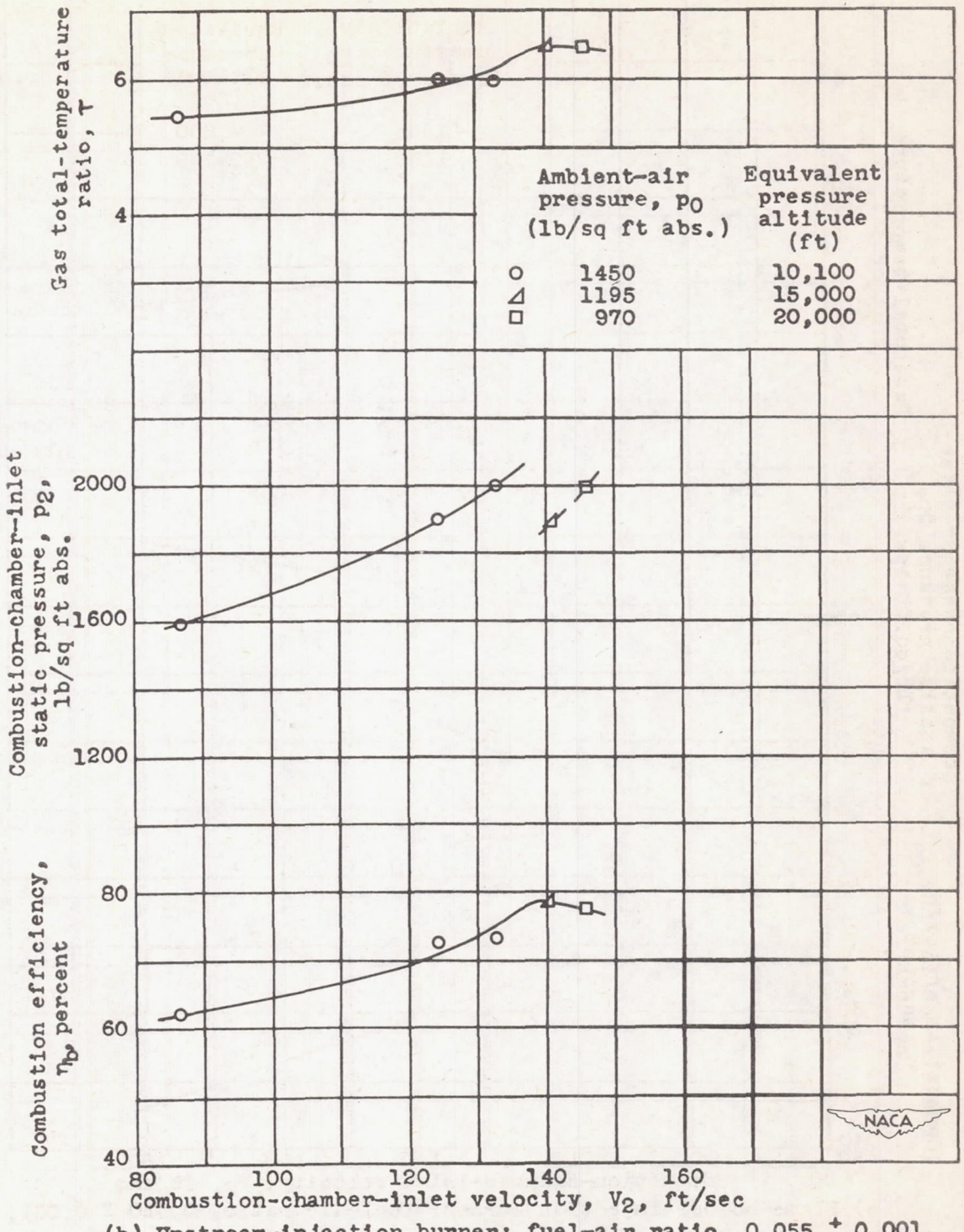

(b) Upstream-injection burner; fuel-air ratio, 0.055 ± 0.001.

Figure 6. - Continued. Effect of combustion-chamber-inlet velocity on combustion efficiency and gas total-temperature ratio at various conditions of ambient-air pressure and combustion-chamber-inlet static pressure. 20-inch ram jet with 8-foot combustion chamber and 17-inch-diameter exhaust nozzle.

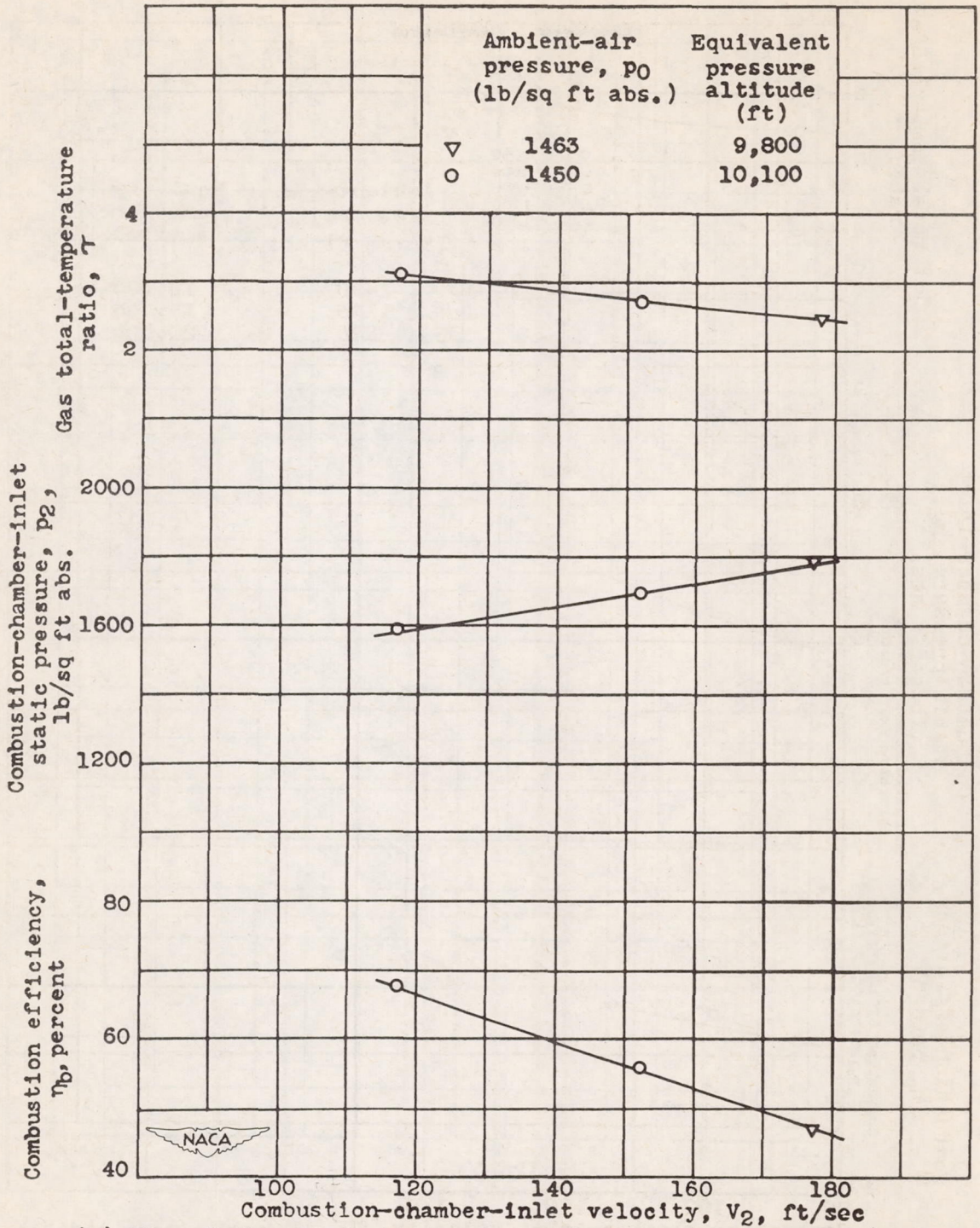

(c) Flame-holder injection burner; fuel-air ratio, 0.020 ± 0.001.

Figure 6. - Concluded. Effect of combustion-chamber-inlet velocity on combustion efficiency and gas total-temperature ratio at various conditions of ambient-air pressure and combustion-chamber-inlet static pressure. 20-inch ram jet with 8-foot combustion chamber and 17-inch-diameter exhaust nozzle.

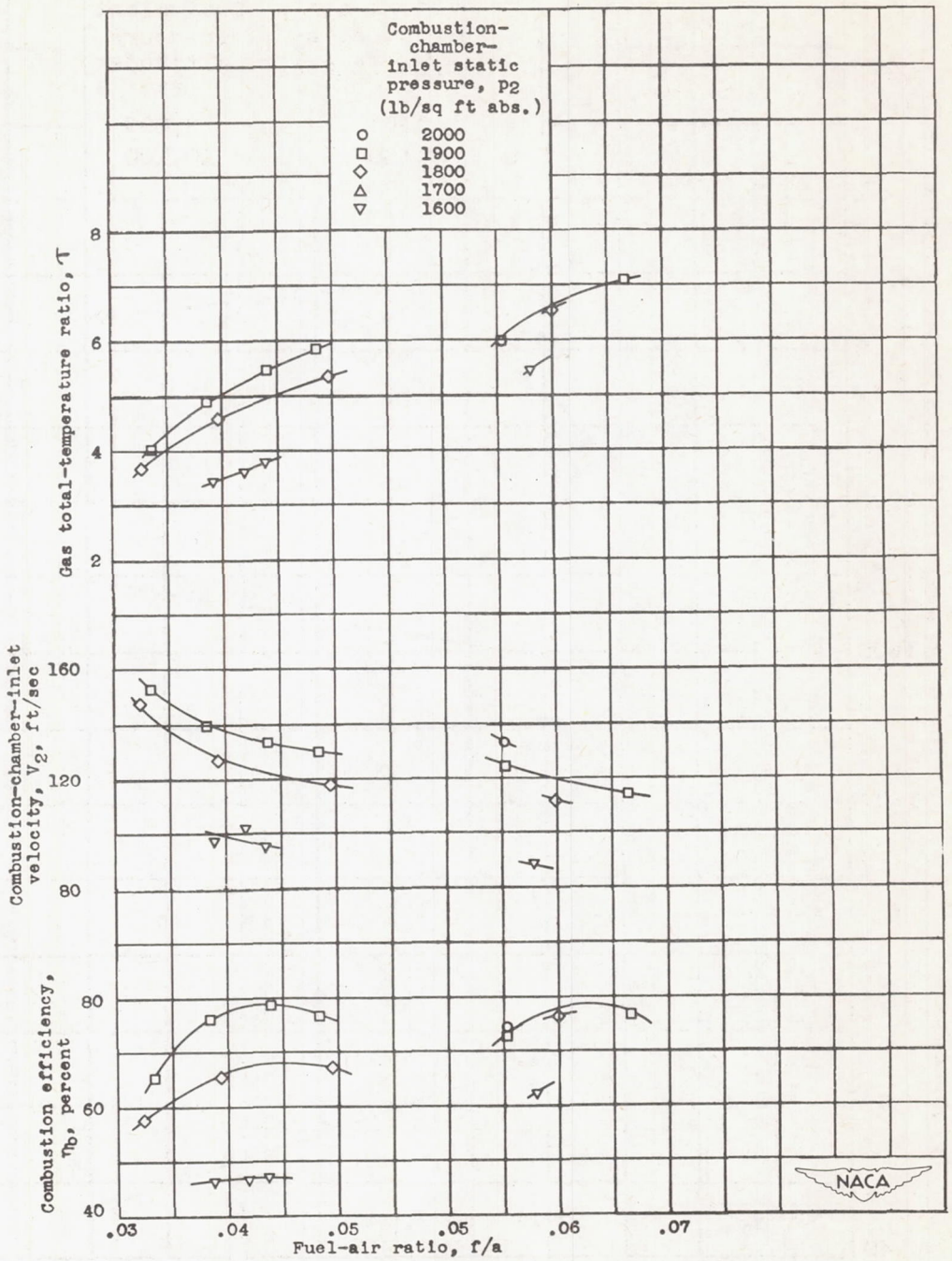

(a) Split-injection burner. (b) Upstream-injection burner.

Figure 7. - Effect of fuel-air ratio on combustion efficiency and gas total-temperature ratio at various conditions of combustion-chamber-inlet velocity and static pressure. 20-inch ram jet with 8-foot combustion chamber and 17-inch-diameter exhaust nozzle; ambient-air pressure, 1450 pounds per square foot absolute, equivalent pressure altitude, 10,100 feet.

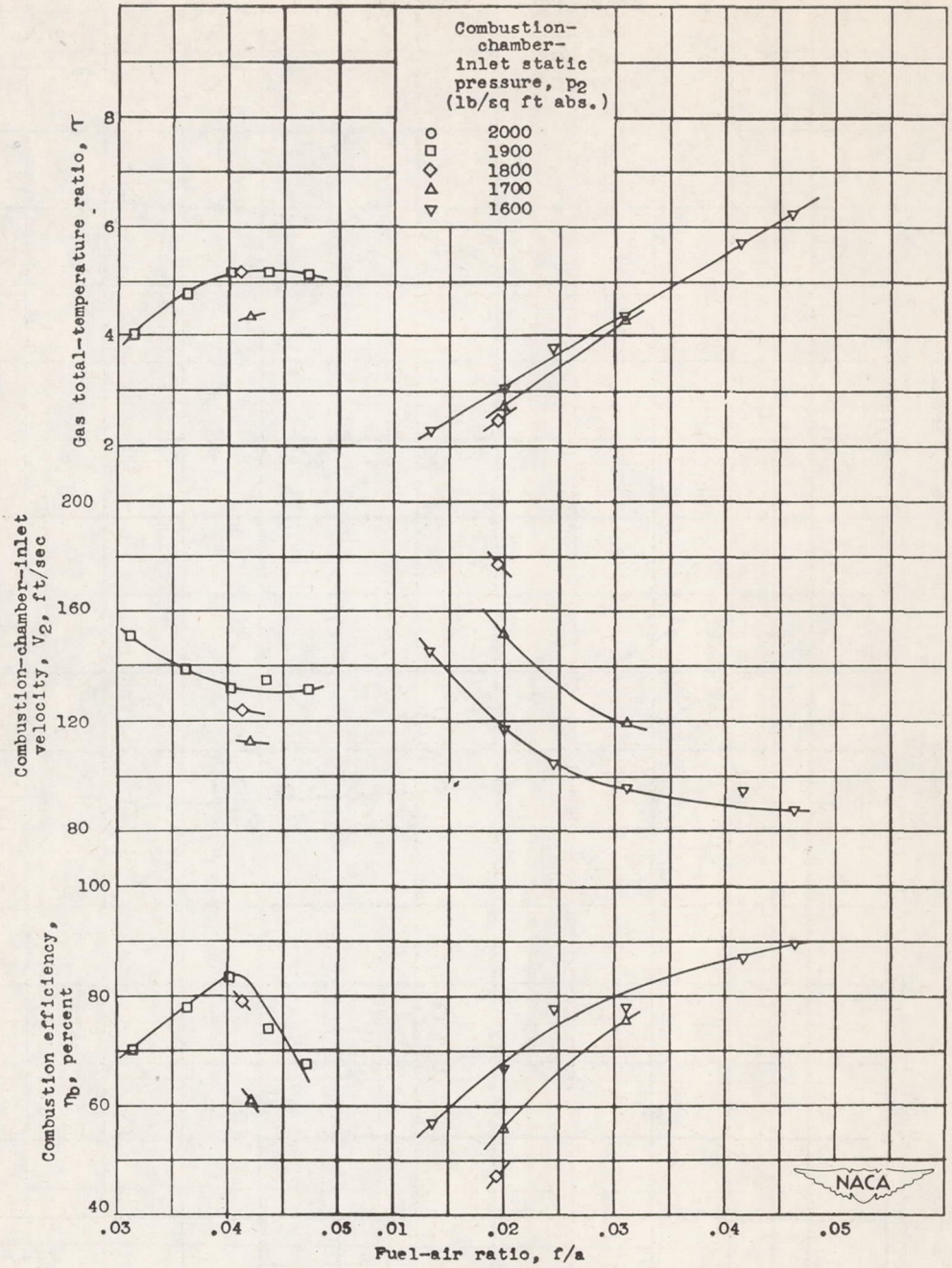

(c) Flame-holder split-injection burner.

(d) Flame-holder injection burner.

Figure 7. - Concluded. Effect of fuel-air ratio on combustion efficiency and gas total-temperature ratio at various conditions of combustion-chamber-inlet velocity and static pressure. 20-inch ram jet with 8-foot combustion chamber and 17-inch-diameter exhaust nozzle; ambient-air pressure, 1450 pounds per square foot absolute; equivalent pressure altitude, 10,100 feet.

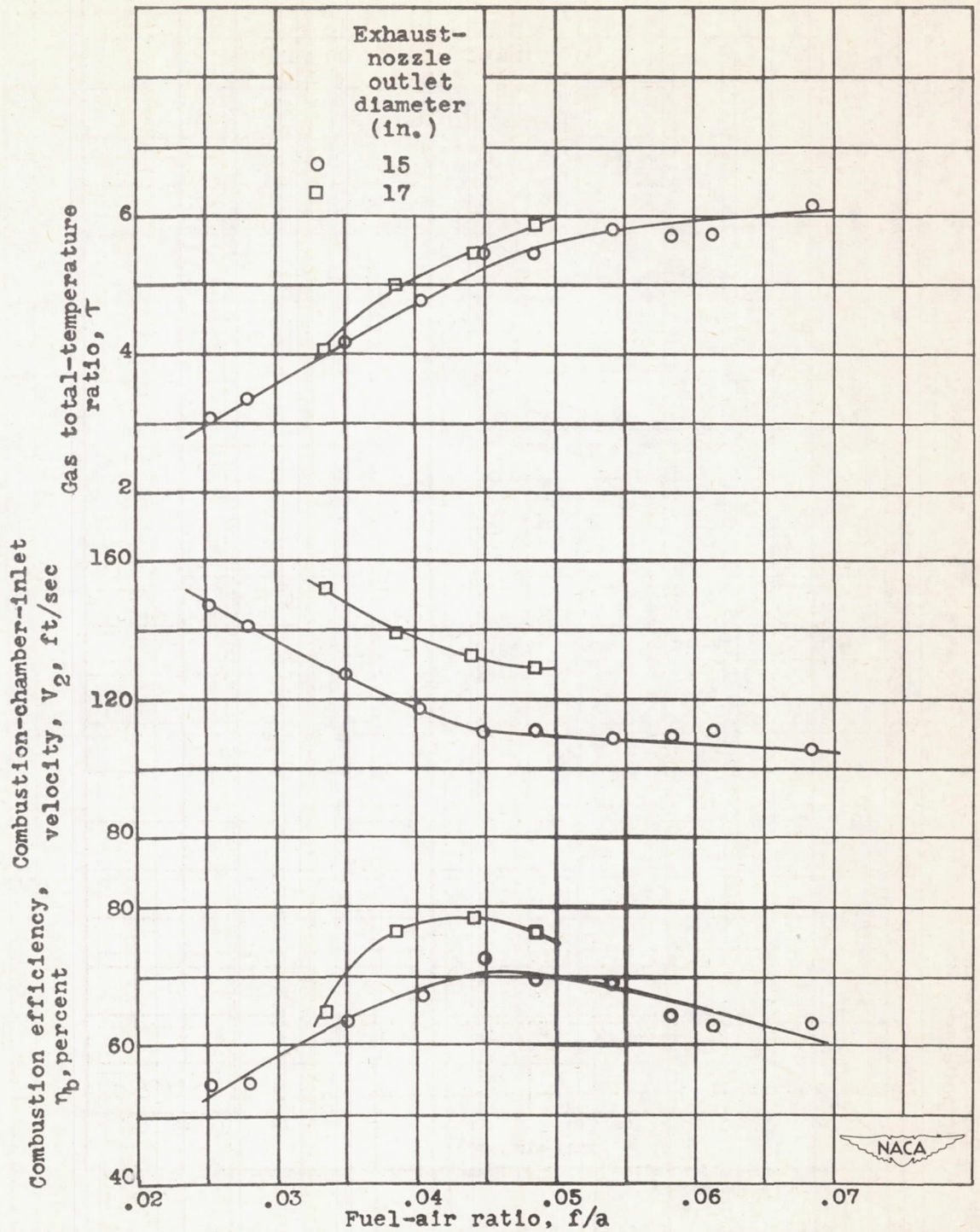

Figure 8. - Effect of fuel-air ratio and exhaust-nozzle-outlet diameter on combustion efficiency, combustion-chamber-inlet velocity, and gas total-temperature ratio. 20-inch ram jet with 8-foot combustion chamber; split-injection burner; ambient-air pressure, 1450 pounds per square foot absolute; equivalent pressure altitude, 10,100 feet; combustion-chamber-inlet static pressure, 1950 ± 50 pounds per square foot.

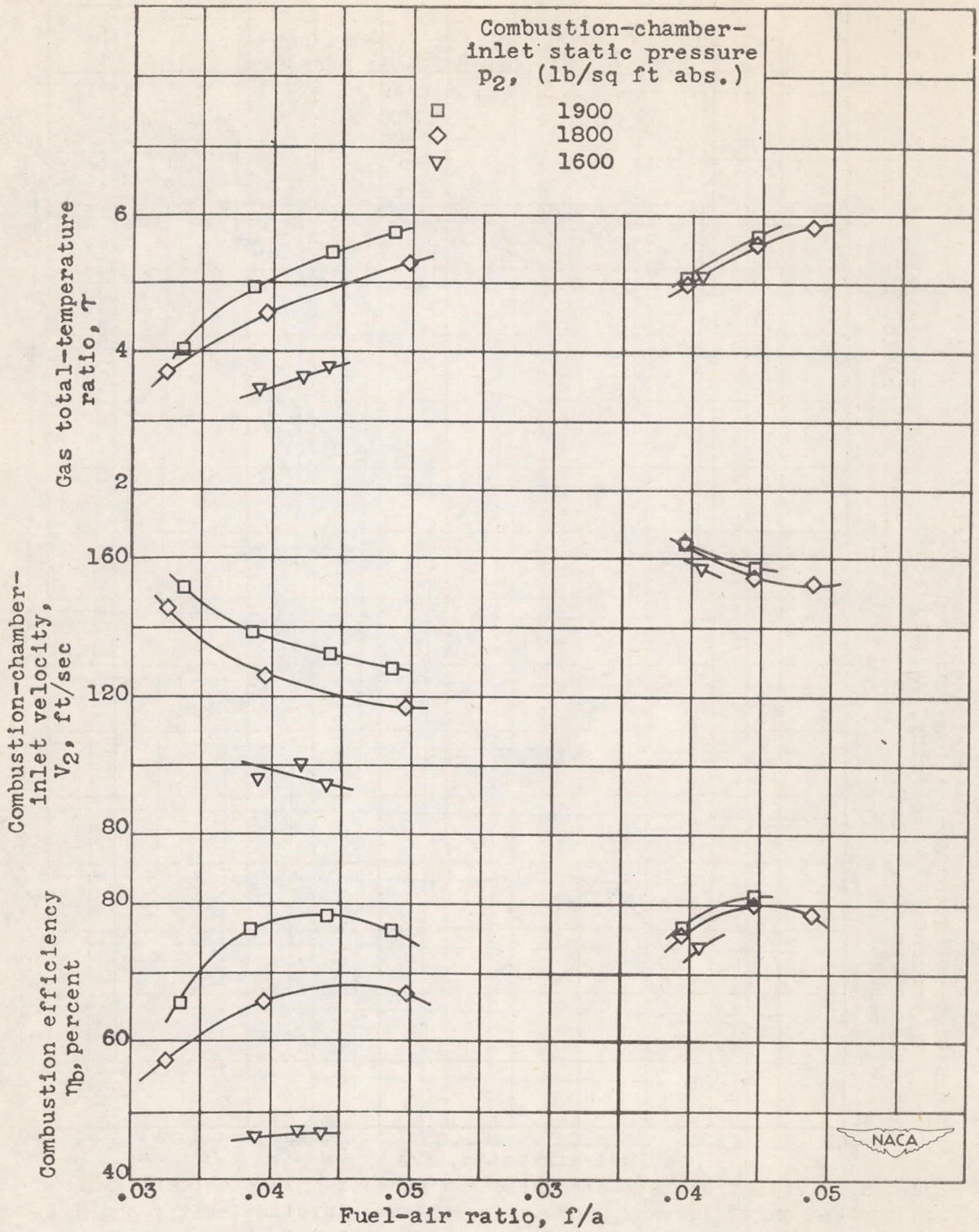

(a) M_0, 0.39 to 0.67; p_0, 1450 pounds per square foot absolute.

(b) M_0, 0.90 to 1.06; p_0, 970 pounds per square foot absolute.

Figure 9. - Effect of exhaust-nozzle choking on combustion-chamber performance. 20-inch ram jet with 8-foot combustion chamber and 17-inch-diameter exhaust nozzle; split-injection burner.

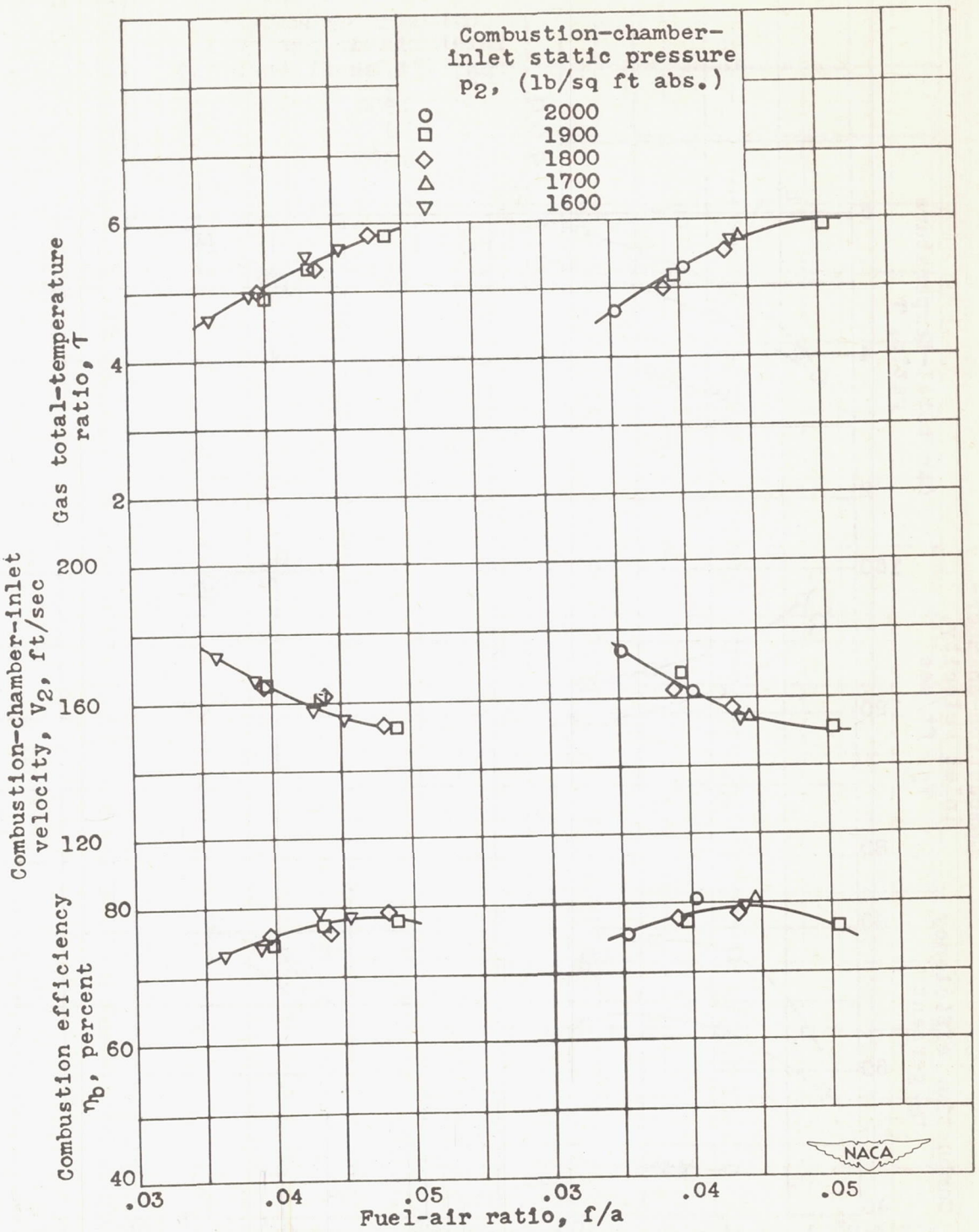

(c) M_0, 1.26 to 1.34; p_0, 630 pounds per square foot absolute.

(d) M_0, 1.44 to 1.60; p_0, 500 pounds per square foot absolute.

Figure 9. - Concluded. Effect of exhaust-nozzle choking on combustion-chamber performance. 20-inch ram jet with 8-foot combustion chamber and 17-inch-diameter exhaust nozzle; split-injection burner.

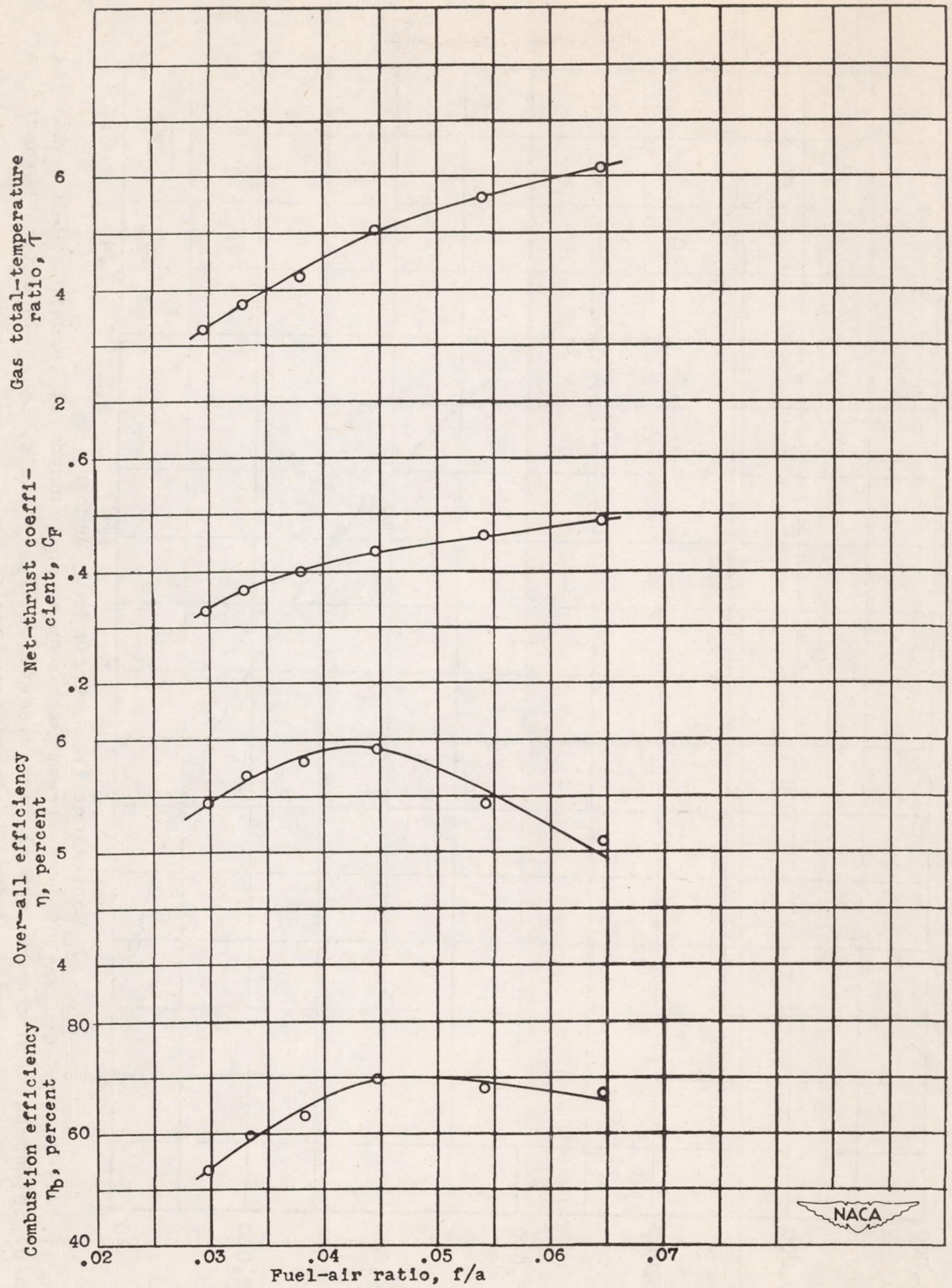

Figure 10. - Effect of fuel-air ratio on combustion efficiency, over-all efficiency, net thrust coefficient, and gas total-temperature ratio. 20-inch ram jet with 8-foot combustion chamber and 15-inch-diameter exhaust nozzle; split-injection burner; equivalent free-stream Mach number M_0, 1.08.

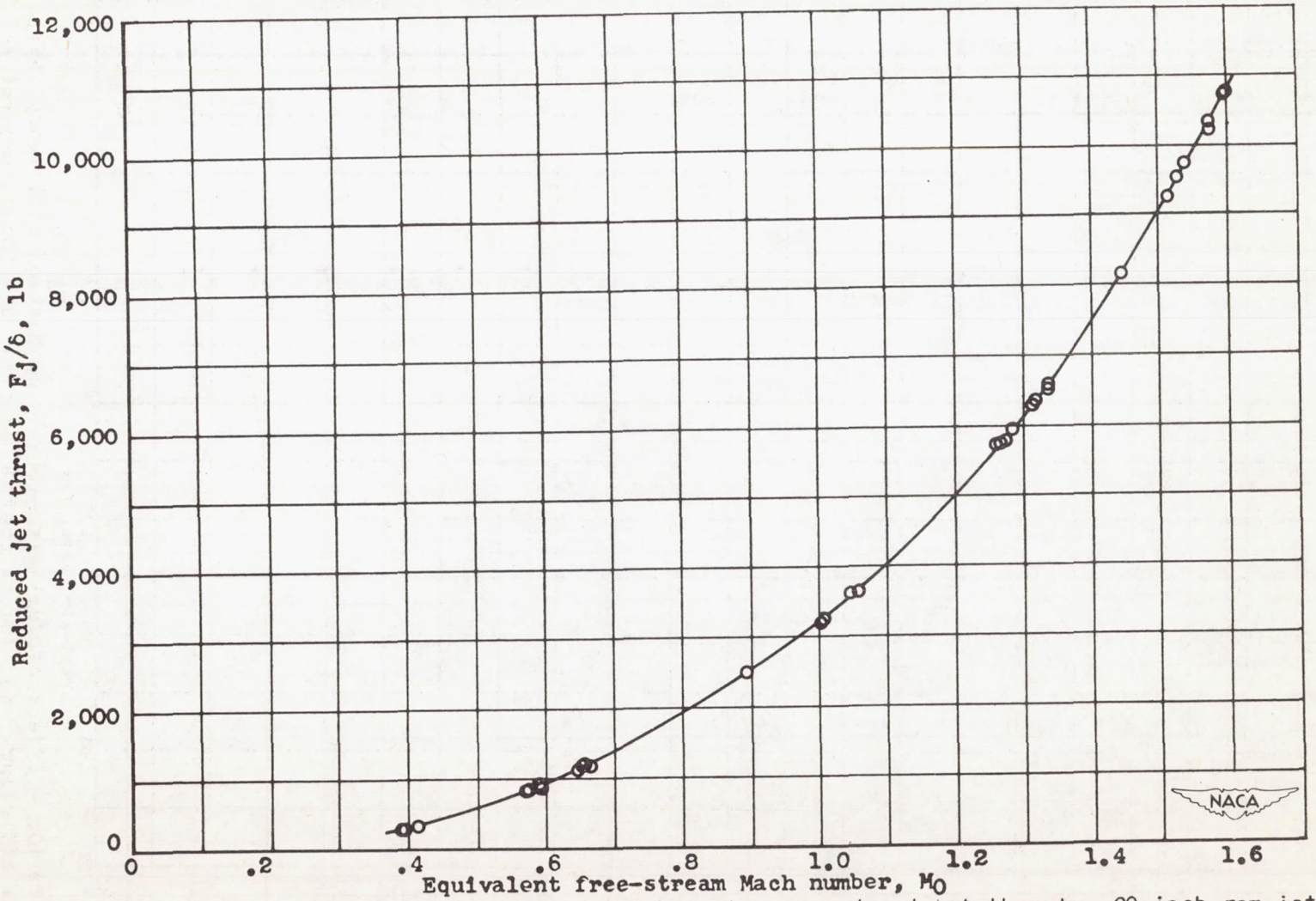

Figure 11. - Effect of equivalent free-stream Mach number on reduced jet thrust. 20-inch ram jet with 8-foot combustion chamber and 17-inch-diameter exhaust nozzle; split-injection burner. Jet thrust reduced to NACA standard conditions at sea level.

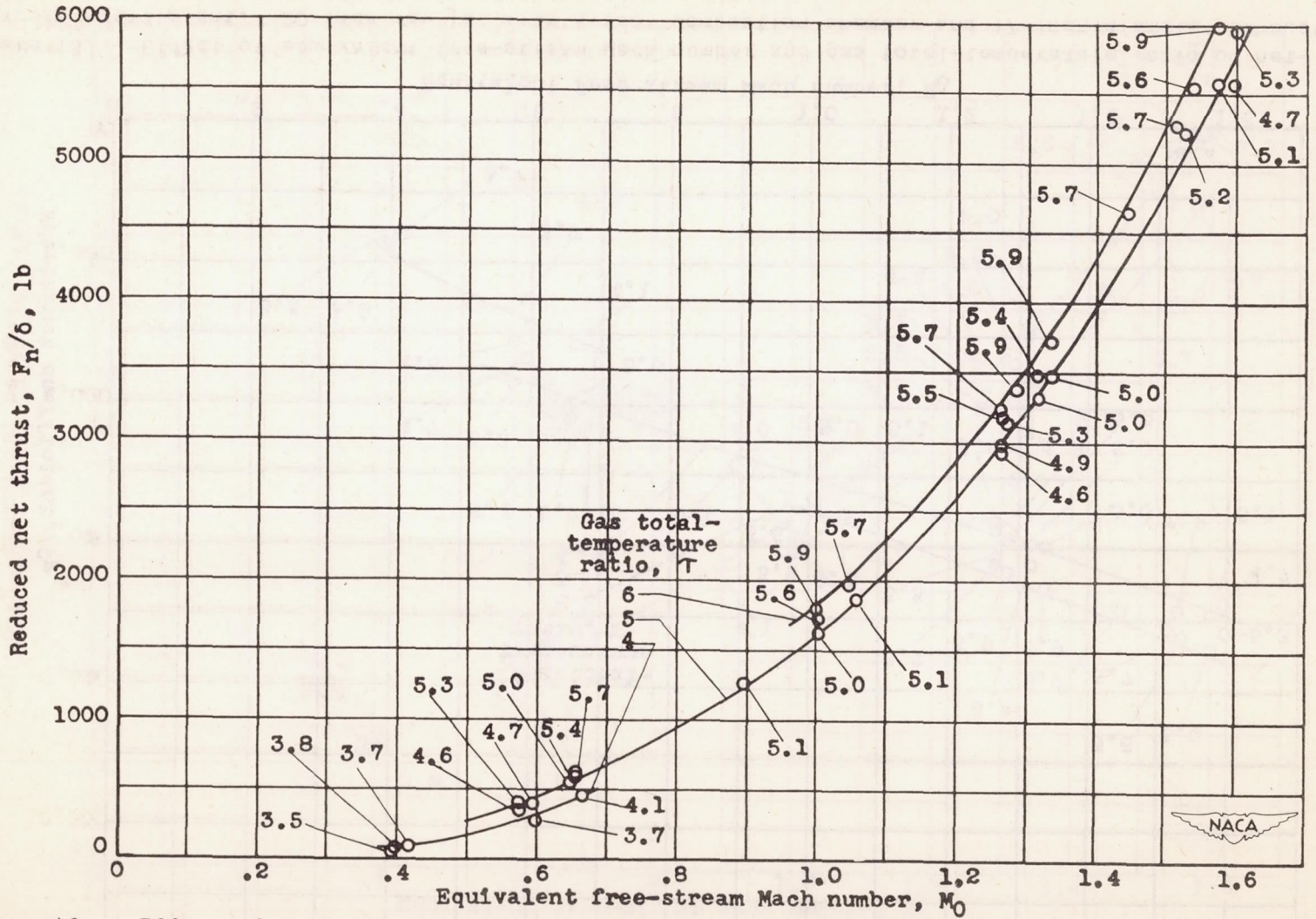

Figure 12. - Effect of equivalent free-stream Mach number and gas total-temperature ratio on reduced net thrust. 20-inch ram jet with 8-foot combustion chamber and 17-inch-diameter exhaust nozzle; split-injection burner. Net thrust reduced to NACA standard conditions at sea level.

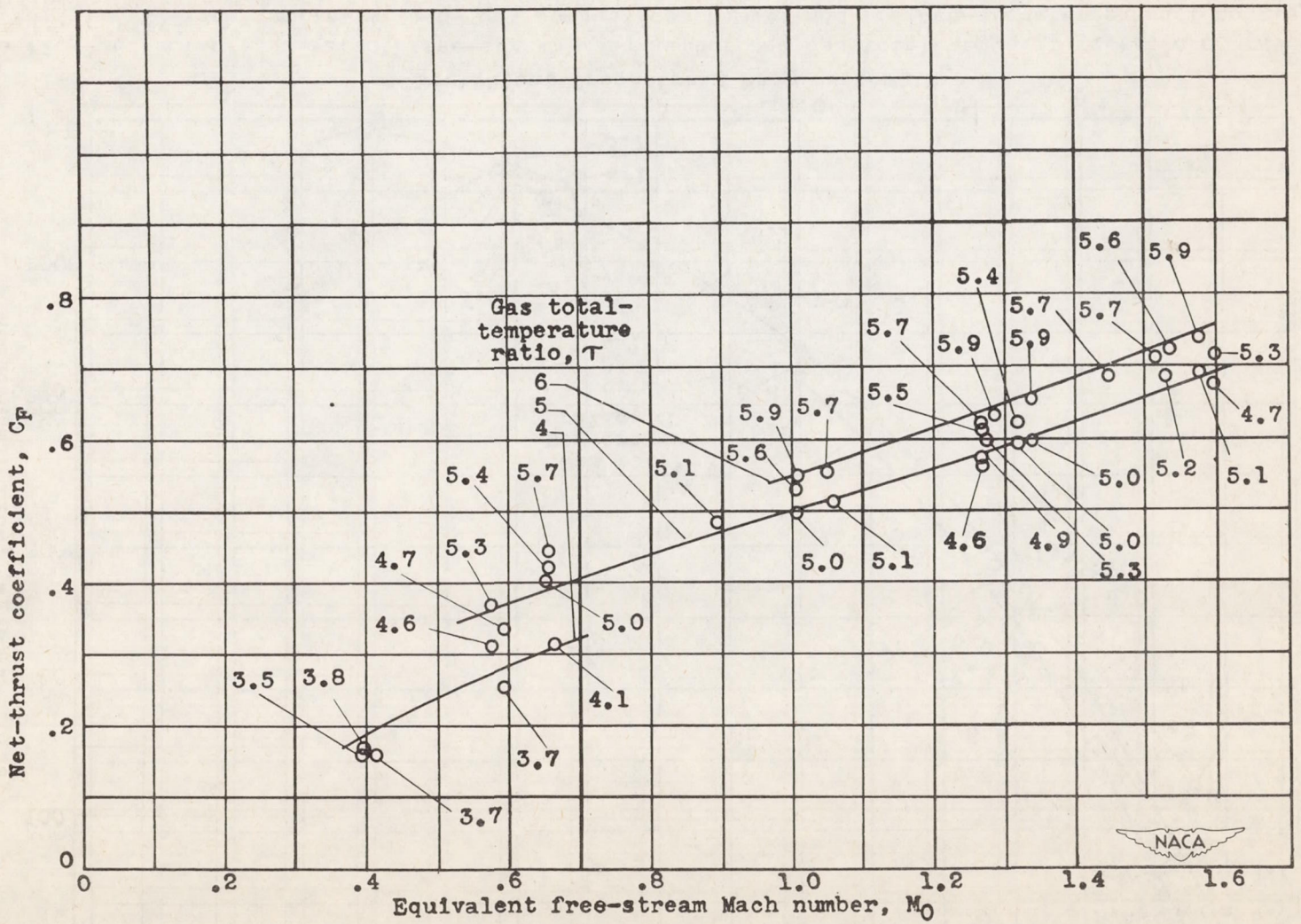

Figure 13. - Effect of equivalent free-stream Mach number and gas total-temperature ratio on net-thrust coefficient. 20-inch ram jet with 8-foot combustion chamber and 17-inch-diameter exhaust nozzle; split-injection burner.

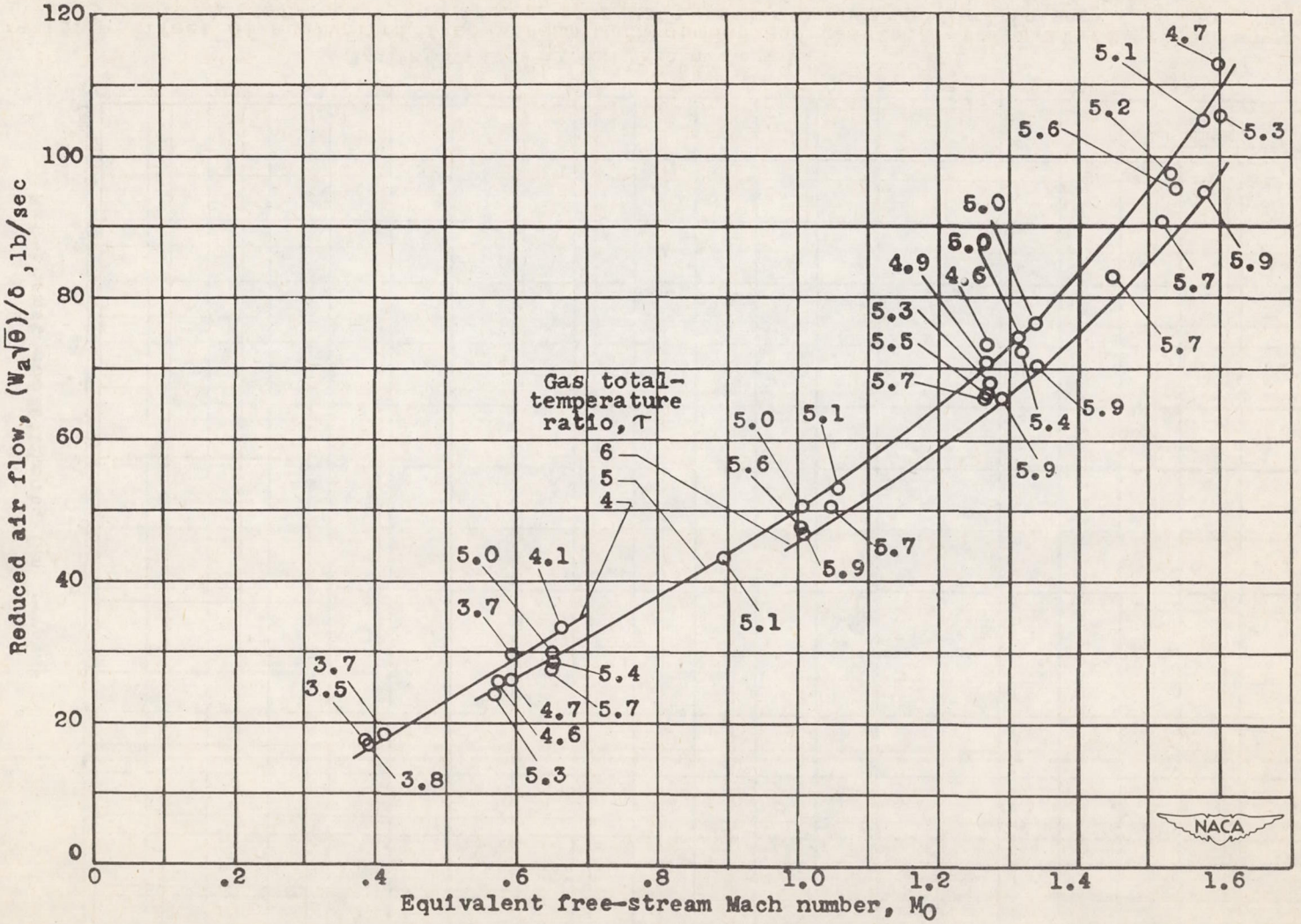

Figure 14. - Effect of equivalent free-stream Mach number and gas-total-temperature ratio on reduced air flow. 20-inch ram jet with 8-foot combustion chamber and 17-inch-diameter exhaust nozzle; split-injection burner. Air flow reduced to NACA standard conditions at sea level.

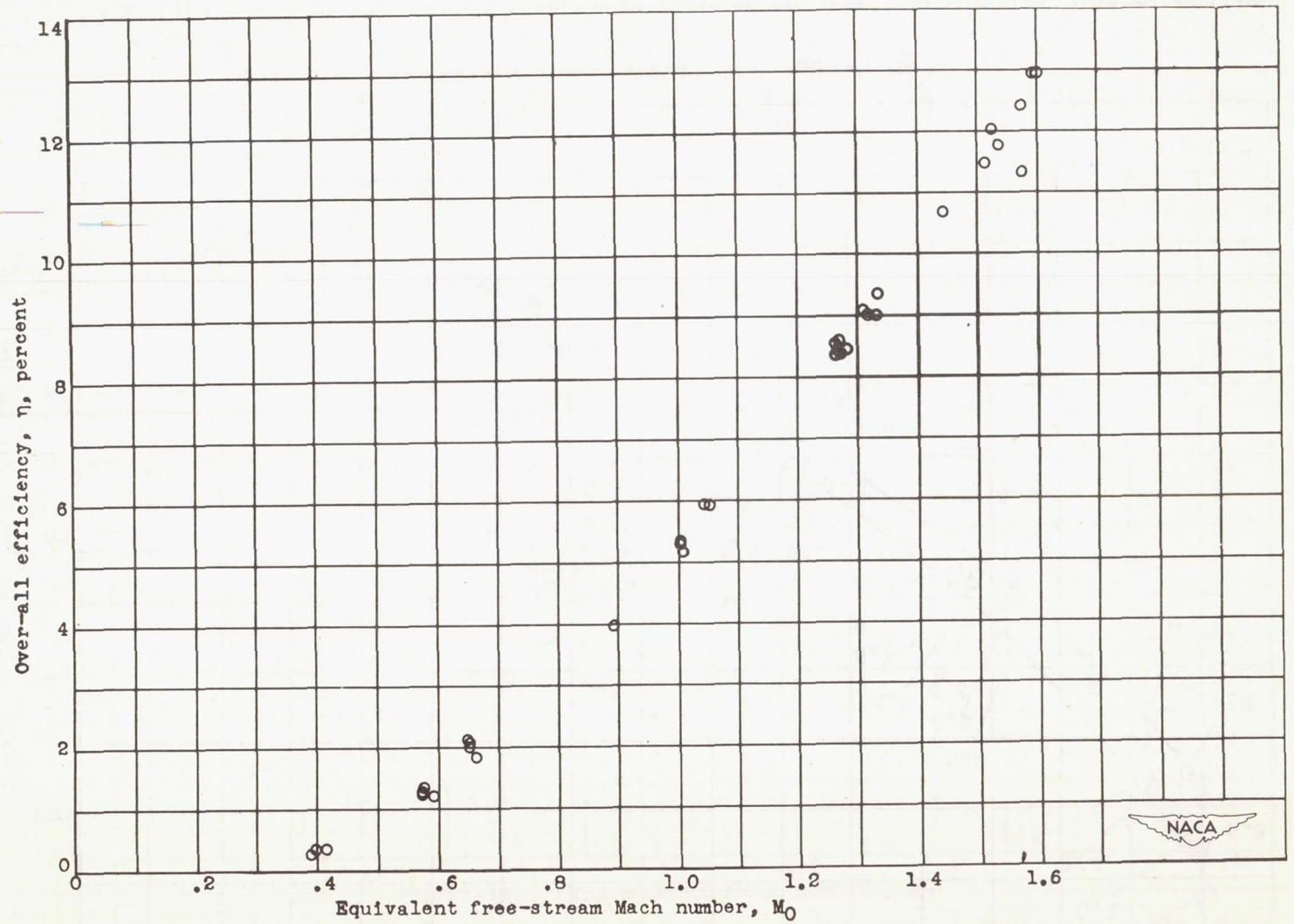

Figure 15. - Effect of equivalent free-stream Mach number on over-all efficiency. 20-inch ram jet with 8-foot combustion chamber and 17-inch-diameter exhaust nozzle; split-injection burner.

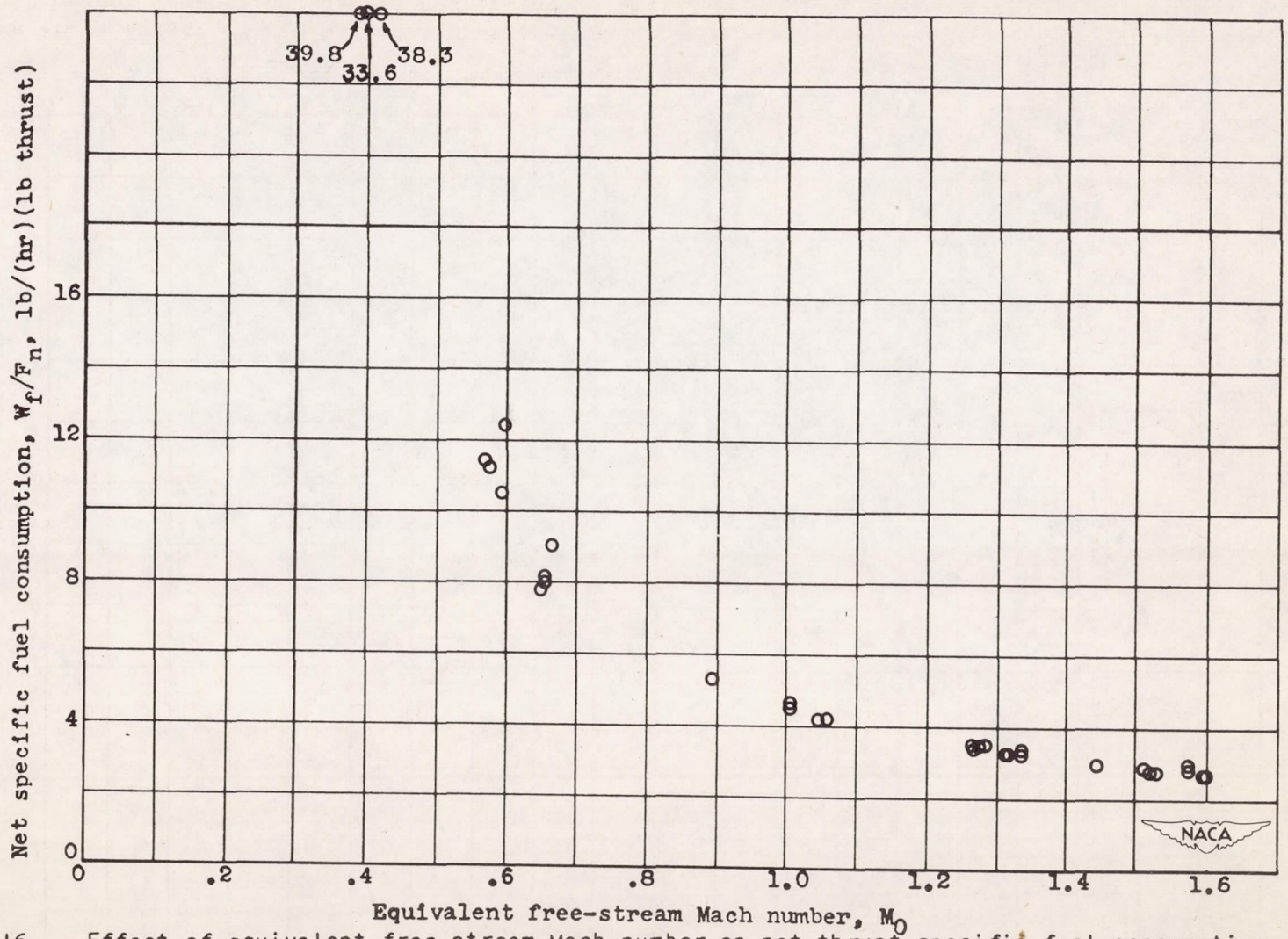

Figure 16. - Effect of equivalent free-stream Mach number on net thrust specific fuel consumption. 20-inch ram jet with 8-foot combustion chamber and 17-inch-diameter exhaust nozzle; split-injection burner.